Journal of Computational Physics 363 (2018) 302–328

Contents lists available at ScienceDirect

Journal of Computational Physics

www.elsevier.com/locate/jcp

Galerkin methods for Boltzmann–Poisson transport with reflection conditions on rough boundaries

José A. Morales Escalante [a,*], Irene M. Gamba [b]

[a] TU Wien – Institute for Analysis and Scientific Computing, Austria
[b] The University of Texas at Austin – Institute for Computational Engineering and Sciences & Department of Mathematics, United States

ARTICLE INFO

Article history:
Received 9 October 2017
Received in revised form 5 February 2018
Accepted 22 February 2018
Available online 27 February 2018

Keywords:
Galerkin
Boltzmann–Poisson
Boundary
Reflection
Diffusive
Specular

ABSTRACT

We consider in this paper the mathematical and numerical modeling of reflective boundary conditions (BC) associated to Boltzmann–Poisson systems, including diffusive reflection in addition to specularity, in the context of electron transport in semiconductor device modeling at nano scales, and their implementation in Discontinuous Galerkin (DG) schemes. We study these BC on the physical boundaries of the device and develop a numerical approximation to model an insulating boundary condition, or equivalently, a pointwise zero flux mathematical condition for the electron transport equation. Such condition balances the incident and reflective momentum flux at the microscopic level, pointwise at the boundary, in the case of a more general mixed reflection with momentum dependant specularity probability $p(\vec{k})$. We compare the computational prediction of physical observables given by the numerical implementation of these different reflection conditions in our DG scheme for BP models, and observe that the diffusive condition influences the kinetic moments over the whole domain in position space.

1. Introduction

The dynamics of electronic transport in modern semiconductor devices can be described by the semiclassical Boltzmann–Poisson (BP) model

$$\frac{\partial f_i}{\partial t} + \frac{1}{\hbar}\nabla_{\vec{k}}\,\varepsilon_i \cdot \nabla_{\vec{x}} f_i - \frac{q_i}{\hbar}\vec{E}\cdot\nabla_{\vec{k}} f_i = \sum_j Q_{i,j}, \tag{1.1}$$

$$\nabla_{\vec{x}}\cdot(\epsilon\,\nabla_{\vec{x}} V) = \sum_i q_i\rho_i - N(\vec{x}), \quad \vec{E} = -\nabla_{\vec{x}} V, \tag{1.2}$$

where $f_i(\vec{x},\vec{k},t)$ is the probability density function (pdf) over phase space $(\vec{x},\vec{k})$ of a carrier in the i-th energy band in position $\vec{x}$, with crystal momentum $\hbar\vec{k}$ at time t. The collision operators $Q_{i,j}(f_i, f_j)$ model i-th and j-th carrier recombinations, collisions with phonons or generation effects. $\vec{E}(\vec{x},t)$ is the electric field, $V(\vec{x},t)$ is the electric potential, $\varepsilon_i(\vec{k})$ is the i-th energy band surface, the i-th charge density $\rho_i(t,\vec{x})$ is the k-average of f_i, $-q_i$ is the electric charge of the i-th carrier, $N(\vec{x})$ is the doping profile, and ϵ is the electric permittivity of the material.

* Corresponding author.
E-mail addresses: jose.morales.escalante@tuwien.ac.at (J.A. Morales Escalante), gamba@math.utexas.edu (I.M. Gamba).

https://doi.org/10.1016/j.jcp.2018.02.041
0021-9991/

The BP model for electron transport on a single conduction energy band for electrons has the form

$$\frac{\partial f}{\partial t} + \frac{1}{\hbar}\nabla_{\vec{k}}\,\varepsilon(\vec{k})\cdot\nabla_{\vec{x}} f - \frac{q}{\hbar}\vec{E}(\vec{x},t)\cdot\nabla_{\vec{k}} f = Q(f), \tag{1.3}$$

$$\nabla_{\vec{x}}\cdot(\epsilon\,\nabla_{\vec{x}} V) = q\left[\rho(\vec{x},t) - N(\vec{x})\right], \quad \vec{E} = -\nabla_{\vec{x}} V, \tag{1.4}$$

with the quantum mechanical electron group velocity $\frac{1}{\hbar}\nabla_{\vec{k}}\,\varepsilon(\vec{k})$, and the electron density $\rho(\vec{x},t) = \int_{\Omega_{\vec{k}}} f(\vec{x},\vec{k},t)\,d\vec{k}$. The collision integral operator $Q(f)$ describes the scattering over the electrons, where several mechanisms of quantum nature can be taken into account. In the low density regime, the collisional integral operator can be approximated as linear in f, having the form

$$Q(f) = \int_{\Omega_{\vec{k}}} \left[S(\vec{k}',\vec{k})\,f(t,\vec{x},\vec{k}') - S(\vec{k},\vec{k}')\,f(t,\vec{x},\vec{k})\right] d\vec{k}', \tag{1.5}$$

where $S(\vec{k},\vec{k}')$ is the scattering kernel, representing non-local interactions of electrons with a background density distribution. For example, in the case of silicon, one of the most important collision mechanisms are electron–phonon scatterings due to lattice vibrations of the crystal, which are modeled by acoustic (assumed elastic) and optical (non-elastic) non-polar modes, the latter with a single frequency ω_p, given by

$$\begin{aligned} S(\vec{k},\vec{k}') = {} & (n_q+1)\,K\,\delta(\varepsilon(\vec{k}') - \varepsilon(\vec{k}) + \hbar\omega_p) \\ & + n_q\,K\,\delta(\varepsilon(\vec{k}') - \varepsilon(\vec{k}) - \hbar\omega_p) + K_0\,\delta(\varepsilon(\vec{k}') - \varepsilon(\vec{k}))\,, \end{aligned} \tag{1.6}$$

with K, K_0 constants for silicon. The symbol δ indicates the usual Dirac delta distribution corresponding to the well known Fermi's Golden Rule [13]. The constant n_q is related to the phonon occupation factor

$$n_q = \left[\exp\left(\frac{\hbar\omega_p}{K_B T_L}\right) - 1\right]^{-1},$$

where K_B is the Boltzmann constant and $T_L = 300$ K is the lattice temperature.

The semi-classical Boltzmann description of electron transport in semiconductors is, for a truly 3-D device, an equation in six dimensions plus time when the device is not in steady state. The heavy computational cost is the main reason why the BP system had been traditionally solved numerically by means of Direct Simulation Monte Carlo (DSMC) methods [14]. However, after the pioneer work [15], in recent years, deterministic solvers to the BP system were proposed in [16–22]. These methods provide accurate results which, in general, agree well with those obtained from Monte Carlo (DSMC) simulations, often at a fractional computational time. Moreover, these type of solvers can resolve transient details for the electron probability density function f, which are difficult to compute with DSMC simulators.

The initial methods proposed in [18–21] using weighted essentially non-oscillatory (WENO) finite difference schemes to solve the Boltzmann–Poisson system, had the advantage that the scheme is relatively simple to code and very stable even on coarse meshes for solutions containing sharp gradient regions. However, a disadvantage of the WENO methods is that it requires smooth meshes to achieve high order accuracy, hence it is not very flexible for adaptive meshes.

Motivated by the easy *hp*-adaptivity and the simple communication pattern of the discontinuous Galerkin (DG) methods for macroscopic (fluid level) models [23–26], it was proposed in [27,28] to implement a DG solver to the full Boltzmann equation, that is capable of capturing transients of the probability density function.

In the previous work [27,28], the first DG solver for (1.1)–(1.2) was proposed, and some numerical calculations were shown for one and two-dimensional devices. In [29], the DG-LDG scheme for the Boltzmann–Poisson system was carefully formulated, and extensive numerical studies were performed to validate the calculations. Such scheme models electron transport along the conduction band for 1D diodes and 2D double gate MOSFET devices with an analytic Kane energy band model.

A DG method for full conduction bands BP models was proposed in [30], following the lines of the schemes in [27–29], generalizing the solver that uses the Kane non-parabolic band and adapting it to treat the full energy band case. A preliminary benchmark of numerical results shows that the direct evaluation of the Dirac delta function can be avoided, and so an accurate high-order simulation with comparable computational cost to the analytic band cases is possible. It would be more difficult or even unpractical to produce the full band computation with other transport scheme. It is worth to notice that a high-order positivity-preserving DG scheme for linear Vlasov–Boltzmann transport equations, under the action of quadratically confined electrostatic potentials, independent of the electron distribution, has been developed in [31]. The authors there show that these DG schemes conserve mass and preserve the positivity of the solution without sacrificing accuracy. In addition, the standard semi-discrete schemes were studied showing stability and error estimates.

The type of DG method discussed in this paper, as was done in [29], belongs to a class of finite element methods originally devised to solve hyperbolic conservation laws containing only first order spatial derivatives, e.g. [32–36]. Using a piecewise polynomial space for both the test and trial functions in the spatial variables, and coupled with explicit and

nonlinearly stable high order Runge–Kutta time discretization, the DG method is a conservative scheme that has the advantage of flexibility for arbitrarily unstructured meshes, with a compact stencil, and with the ability to easily accommodate arbitrary *hp*-adaptivity. For more details about DG scheme for convection dominated problems, we refer to the review paper [37], later generalized to the Local DG (LDG) method to solve the convection diffusion equations [38] and elliptic equations [39].

Regarding Boundary Conditions (BC), there are several kinds of BC for BP semiconductor models. They vary according to the considered device and physical situation. We list below several examples of BC that could arise in the case of electron transport along a single conduction band.

Charge neutrality boundary conditions, given by [4]

$$f_{out}(t,\vec{x},\vec{k})\Big|_{\Gamma} = N_D(\vec{x})\left.\frac{f_{in}(t,\vec{x},\vec{k})}{\rho_{in}(t,\vec{x})}\right|_{\Gamma}, \quad \Gamma \quad \text{subset of } \partial\Omega_{\vec{x}}, \tag{1.7}$$

where $\Omega_{\vec{x}}$ is the position domain. This BC is imposed in source and drain boundaries, where electric currents enter or exit the device, to achieve neutral charges there, as $\rho_{out}(\vec{x},t) - N_D(\vec{x}) = 0$.

Reflective BC happen in insulating boundaries, usually defined by a Neumann boundary Γ_N, of 2D and 3D devices. In general, reflective BC can be formulated as the values of the pdf at the inflow boundary being dependent on the outflow boundary values

$$f(\vec{x},\vec{k},t)|_{\Gamma_{N^-}} = F_R\left(f|_{\Gamma_{N^+}}\right), \tag{1.8}$$

$F_R\left(f|_{\Gamma_{N^+}}\right)$ denoting that the reflection boundary condition is a function of the outflow boundary values of the probability density function, where the Neumann Inflow Boundary is defined as

$$\Gamma_N^- = \{(\vec{x},\vec{k}) \,|\, \vec{x}\in\Gamma_N,\ \vec{k}\in\Omega_{\vec{k}},\ \vec{v}(\vec{k})\cdot\eta(\vec{x}) < 0\}, \tag{1.9}$$

$$\vec{v}(\vec{k}) = \frac{1}{\hbar}\nabla_{\vec{k}}\,\varepsilon(\vec{k}), \tag{1.10}$$

with $\Omega_{\vec{k}}$ the momentum domain, $\eta(\vec{x})$ outward unit normal, and the Neumann Outflow Boundary is defined as

$$\Gamma_N^+ = \{(\vec{x},\vec{k}) \,|\, \vec{x}\in\Gamma_N,\ \vec{k}\in\Omega_{\vec{k}},\ \vec{v}(\vec{k})\cdot\eta(\vec{x}) > 0\}. \tag{1.11}$$

Specular Reflection BC over the Neumann Inflow Boundary is given by

$$f|_-(\vec{x},\vec{k},t) = F_S(f|_+) = f|_+(\vec{x},\vec{k}',t) \quad \text{for} \quad (\vec{x},\vec{k})\in\Gamma_N^-, \quad t>0, \tag{1.12}$$

$$(\vec{x},\vec{k}')\in\Gamma_N^+, \quad \vec{k}' \quad \text{s.t.} \quad \vec{v}(\vec{k}') = \vec{v}(\vec{k}) - 2\,\eta(\vec{x})\cdot\vec{v}(\vec{k})\,\eta(\vec{x}). \tag{1.13}$$

Diffusive reflection is a known condition from kinetic theory, in which the distribution function at the Inflow boundary is proportional to a Maxwellian [1], [2] with $T = T_W = T_W(\vec{x})$ the temperature at the wall

$$f|_-(\vec{x},\vec{k},t) = F_D(f|_+) = C\,\sigma\left\{f|_+\right\}(\vec{x},t)\,e^{-\varepsilon(\vec{k})/K_BT}, \quad (\vec{x},\vec{k})\in\Gamma_N^-, \tag{1.14}$$

$$\sigma\left\{f|_+\right\}(\vec{x},t) = \int\limits_{\vec{v}(\vec{k})\cdot\eta>0} \vec{v}(\vec{k})\cdot\eta(\vec{x})\,f|_+(\vec{x},\vec{k},t)dk, \tag{1.15}$$

$$C = C\left\{\eta(\vec{x})\right\} = \left(\int\limits_{\vec{v}\cdot\eta<0} |\vec{v}\cdot\eta|\,e^{-\varepsilon(\vec{k})/K_BT_L}\,d\vec{k}\right)^{-1}.$$

Mixed reflection BC models the effect of a physical surface on electron transport in metals and semiconductors, giving the reflected pdf representing the electrons as a linear convex combination of specular and diffuse components, as in the formula

$$\begin{aligned} f|_-(\vec{x},\vec{k},t) &= F_M(f|_+) = p\,F_S(f|_+) + (1-p)\,F_D(f|_+) \\ &= p\,f|_+(\vec{x},\vec{k}',t) + (1-p)\,C'\sigma'\left\{f|_+\right\}(\vec{x},t)\,e^{-\frac{\varepsilon(\vec{k})}{K_BT}}, \quad (\vec{x},\vec{k})\in\Gamma_N^-. \end{aligned} \tag{1.16}$$

p is sometimes called specularity parameter. It can either be constant or a function, dependant of the momentum. For example, the work by Soffer [5] studies a statistical model for the reflection from a rough surface in electrical conduction. It derives a specularity parameter $p(\vec{k})$ which depends on the momentum, given by

$$p(\vec{k}) = e^{-4l_r^2|k|^2\cos^2\Theta}, \tag{1.17}$$

where l_r is the rms height of the rough interface, and Θ is th angle between the incident electron and the interface surface normal.

Reflection BC is a widely studied topic in the context of the kinetic theory of gases modeled by Boltzmann Equations. However, in the context of kinetic models for electron transport in semiconductors, there is less extensive previous work related to the study of the effect of reflection boundary conditions such as diffusive, specular, or mixed reflection. An example of the list of references where reflection BC are studied for Boltzmann equations in the context of kinetic theory of gases would include the works of Cercignani [3] and Sone [1], where the specular, diffusive, and mixed reflection BC are formulated for the Boltzmann Eq. for gases. V. D. Borman, S. Yu. Krylov, A. V. Chayanov [9] study the nonequilibrium phenomena at a gas-solid interface. The recent paper of Brull, Charrier, Mieussens [10] studies the gas-surface interaction at a nano-scale and the boundary conditions for the associated Boltzmann equation. The recent work of Struchtrup [11] studies as well the Maxwell boundary condition and velocity dependent accommodation coefficients in the context of gases mentioned. It considers the convex combination of specular reflection, isotropic scattering, and diffusive reflection, incorporating velocity dependent coefficients into a Maxwell-type reflection kernel. It develops a modification of Maxwell's BC, extending the Maxwell model by allowing it to incorporate velocity dependent accommodation coefficients into the microscopic description and satisfying conditions of reciprocity and unitary probability normalization.

Regarding reflectivity in the context of Boltzmann models of electron transport, Fuchs [6] proposed a boundary condition for the probability density function of free electrons incident in the material surface, which is a convex combination of specular & diffuse reflection with a constant specularity parameter p. Greene ([7], [8]) studied conditions for the Fuchs BC in which the specularity parameter $p(\vec{k})$ is dependant on the angle of the momentum $\vec{k}$, deriving a boundary condition for electron distributions at crystal surfaces valid for metal, semimetal, & semiconductor surfaces, and showing that Fuchs' reflectivity parameter differs from the kinetic specularity parameter in physical significance and in magnitude. It considers the unperturbed electron states of a crystal with an ideal perfectly specular surface as standing wave states, and the diffusive reflection killing partially the incoming wave function. Soffer [5] studies a statistical model for the electrical conduction, and derives under certain assumptions, such as a rough surface random model with a Gaussian probability of height above or below a horizontal plane, analytical formulas for a momentum dependant specularity parameter $p(\vec{k}) = \exp(-4l_r^2|k|^2\cos^2\Theta)$ associated to this physical phenomena, abovementioned in (1.17). As mentioned before, l_r is the rms height of rough interface, and Θ is th angle between the incident electron and the interface surface normal.

The reference book of Markowich, Ringhofer, & Schmeiser [12] for semiconductor equations discusses the mathematical definition of boundaries according to the physical phenomena, and defines accordingly the kind of BC to be imposed at those boundaries: Dirichlet, Neumann, Inflow and Outflow boundaries. A work of particular importance for us is the one by Cercignani, Gamba, and Levermore [4]. They study high field approximations to a Boltzmann–Poisson system and boundary conditions in a semiconductor. The BP system for electrons in a semiconductor in the case of high fields and small devices is considered. Boundary conditions are proposed at the kinetic level that yield charge neutrality at ohmic contacts, which are Dirichlet boundaries, and at insulating Neumann boundaries. Both BC, either the one yielding charge neutrality at Dirichlet boundaries, or the one rendering zero flux of electrons at the boundary, assume that the pdf is proportional to a ground state associated to an asymptotic expansion of a dimensionless Boltzmann–Poisson system. Then they study closures of moment equations and BC for both the pdf and for the moment closures. The paper [40] also comments on the study of boundary conditions for kinetic and macroscopic approximations for the Boltzmann–Poisson system in bounded domains. Jüngel mentions in his semiconductors book [2] the different kinds of reflection BC common on the kinetic theory of gases, specular, diffusive, and mixed reflection but no further study of diffusive and mixed reflection BC in the context of semiconductors is pursued.

We intend to present in this work a mathematical, numerical, and computational study of the effect of diffusive, specular, and mixed reflection BC in Boltzmann–Poisson models of electron transport in semiconductors, solved by means of Discontinuous Galerkin FEM solvers. We study the mathematical formulation of these reflection BC in the context of BP models for semiconductors, and derive equivalent numerical formulations of the diffusive and mixed reflection BC with non-constant $p(\vec{k})$, such that an equivalent numerical zero flux condition is satisfied pointwise at the insulating Neumann boundaries at the numerical level. We present numerical simulations for a 2D silicon diode and a 2D double gated MOSFET, comparing the effects of specular, diffusive, and mixed reflection boundary conditions in the physical observable quantities obtained from the simulations.

2. BP system with $\vec{k}$ coordinate transformation assuming a Kane Energy Band

The Kane Energy Band Model is a dispersion relation between the conduction energy band ε (measured from a local minimum) and the norm of the electron wave vector $|k|$, given by the analytical function (α is a constant parameter, m^* is the electron reduced mass for Si, and $\hbar$ is Planck's constant)

$$\varepsilon(1+\alpha\varepsilon) = \frac{\hbar^2|k|^2}{2m^*} \quad . \tag{2.18}$$

For our preliminary numerical studies we will use a Boltzmann–Poisson model as in [29], in which the conduction energy band is assumed to be given by a Kane model. We use the following dimensionalized variables, with the related characteristic parameters

$$t = \mathrm{t}/t_*, (x, y) = \vec{x}/\ell_*, \ell_* = 10^{-6}\ \mathrm{m}, t_* = 10^{-12}\ \mathrm{s}, V_* = 1\ \mathrm{V}.$$

A transformed Boltzmann transport equation is used as in [29] as well, where the coordinates used to describe $\vec{k}$ are: μ, the cosine of the polar angle, the azimuthal angle φ, and the dimensionless Kane Energy $w = \varepsilon/K_B T$, which is assumed as the conduction energy band. We will assume that the wall temperature is equal to the lattice temperature, so $T_W = T = T_L$, and $\alpha_K = \alpha K_B T$. So $\vec{k}(w, \mu, \varphi)$, where

$$\vec{k} = \frac{\sqrt{2m^* K_B T_L}}{\hbar}\sqrt{w(1+\alpha_K w)}\left(\mu, \sqrt{1-\mu^2}\cos\varphi, \sqrt{1-\mu^2}\sin\varphi\right). \tag{2.19}$$

A new unknown function Φ is used in the transformed Boltzmann Eq. [29], which is proportional to the Jacobian of the transformation and to the density of states (up to a constant factor)

$$\Phi(t, x, y, w, \mu, \varphi) = s(w) f(\mathrm{t}, \vec{x}, \vec{k}),$$

where

$$s(w) = \sqrt{w(1+\alpha_K w)}(1+2\alpha_K w). \tag{2.20}$$

The transformed Boltzmann transport equation for Φ used in [29] is

$$\frac{\partial \Phi}{\partial t} + \frac{\partial}{\partial x}(g_1\Phi) + \frac{\partial}{\partial y}(g_2\Phi) + \frac{\partial}{\partial w}(g_3\Phi) + \frac{\partial}{\partial \mu}(g_4\Phi) + \frac{\partial}{\partial \varphi}(g_5\Phi) = C(\Phi). \tag{2.21}$$

The vector (g_1, g_2) represent the 2D Cartesian components of the electron velocity $\frac{1}{\hbar}\nabla_{\vec{k}}\varepsilon(\vec{k})$, in the coordinate system (w, μ, φ). The triplet (g_3, g_4, g_5) represent the transport in the phase space of the new momentum coordinates (w, μ, φ) due to the self consistent electric field

$$\vec{E}(t, x, y) = \big(E_x(t, x, y), E_y(t, x, y), 0\big),$$

with

$$\begin{aligned}
g_1(\cdot) &= c_x \frac{\sqrt{w(1+\alpha_K w)}}{1+2\alpha_K w}\mu,\\
g_2(\cdot) &= c_x \frac{\sqrt{w(1+\alpha_K w)}}{1+2\alpha_K w}\sqrt{1-\mu^2}\cos\varphi,\\
g_3(\cdot) &= -c_k \frac{2\sqrt{w(1+\alpha_K w)}}{1+2\alpha_K w}\left[\mu\, E_x(t, x, y) + \sqrt{1-\mu^2}\cos\varphi\, E_y(t, x, y)\right],\\
&= -c_k \frac{2\sqrt{w(1+\alpha_K w)}}{1+2\alpha_K w}\,\hat{e}_w \cdot \vec{E}(t, x, y),\\
g_4(\cdot) &= -c_k \frac{\sqrt{1-\mu^2}}{\sqrt{w(1+\alpha_K w)}}\left[\sqrt{1-\mu^2}\, E_x(t, x, y) - \mu\cos\varphi\, E_y(t, x, y)\right],\\
&= -c_k \frac{\sqrt{1-\mu^2}}{\sqrt{w(1+\alpha_K w)}}\,\hat{e}_\mu \cdot \vec{E}(t, x, y),\\
g_5(\cdot) &= -c_k \frac{-\sin\varphi}{\sqrt{w(1+\alpha_K w)}\sqrt{1-\mu^2}}\, E_y(t, x, y)\\
&= -c_k \frac{1}{\sqrt{w(1+\alpha_K w)}\sqrt{1-\mu^2}}\,\hat{e}_\varphi \cdot \vec{E}(t, x, y),\\
c_x &= \frac{t_*}{\ell_*}\sqrt{\frac{2\,K_B T_L}{m^*}} \quad \text{and} \quad c_k = \frac{t_* q E_*}{\sqrt{2m^* K_B T_L}},
\end{aligned}$$

and $\hat{e}_w$, $\hat{e}_\mu$, $\hat{e}_\varphi$ the orthonormal vector basis in our momentum coordinate space.

The right hand side of (2.21) is the collision operator (having applied the Dirac Delta's due to electron–phonon scattering, which depend on the energy differences between transitions)

$$C(\Phi)(t,x,y,w,\mu,\varphi) = s(w)\left\{ c_0 \int_0^{\pi} d\varphi' \int_{-1}^{1} d\mu'\, \Phi(t,x,y,w,\mu',\varphi') \right.$$
$$\left. + \int_0^{\pi} d\varphi' \int_{-1}^{1} d\mu' \left[c_+ \Phi(t,x,y,w+\gamma,\mu',\varphi') + c_- \Phi(t,x,y,w-\gamma,\mu',\varphi') \right] \right\}$$
$$- \Phi(t,x,y,w,\mu,\varphi)\, 2\pi \left[c_0 s(w) + c_+ s(w-\gamma) + c_- s(w+\gamma) \right],$$

with the dimensionless parameters

$$(c_0, c_+, c_-) = \frac{2m^* t_*}{\hbar^3} \sqrt{2m^* K_B T_L}\, \big(K_0, (n_q+1)K, n_q K\big), \quad \gamma = \frac{\hbar\omega_p}{K_B T_L}.$$

The electron density is

$$n(t_* t, \ell_* x, \ell_* y) = \int_{\mathbb{R}^3} f(t_* t, \ell_* x, \ell_* y, \mathbf{k})\, d\mathbf{k} = \left(\frac{\sqrt{2m^* K_B T_L}}{\hbar} \right)^3 \rho(t,x,y),$$

where

$$\rho(t,x,y) = \int_0^{+\infty} dw \int_{-1}^{1} d\mu \int_0^{\pi} d\varphi\, \Phi(t,x,y,w,\mu,\varphi). \tag{2.22}$$

Hence, the dimensionless Poisson equation is

$$\frac{\partial}{\partial x}\left(\epsilon_r \frac{\partial \Psi}{\partial x} \right) + \frac{\partial}{\partial y}\left(\epsilon_r \frac{\partial \Psi}{\partial y} \right) = c_p \left[\rho(t,x,y) - \mathcal{N}_D(x,y) \right], \tag{2.23}$$

with

$$\mathcal{N}_D(x,y) = \left(\frac{\sqrt{2m^* K_B T_L}}{\hbar} \right)^{-3} N_D(\ell_* x, \ell_* y) \text{ and } c_p = \left(\frac{\sqrt{2m^* K_B T_L}}{\hbar} \right)^3 \frac{\ell_*^2 q}{\epsilon_0}.$$

3. Discontinuous Galerkin method for transformed Boltzmann–Poisson system and implementation of boundary conditions

The domain of the devices to be considered can be represented by means of a rectangular grid in both position and momentum space. This rectangular grid, bidimensional in position space and tridimensional in momentum space, is defined as

$$\Omega_{ijkmn} = X_{ij} \times K_{kmn},$$
$$X_{ij} = \left[x_{i-\frac{1}{2}}, x_{i+\frac{1}{2}} \right] \times \left[y_{j-\frac{1}{2}}, y_{j+\frac{1}{2}} \right],$$
$$K_{kmn} = \left[w_{k-\frac{1}{2}}, w_{k+\frac{1}{2}} \right] \times \left[\mu_{m-\frac{1}{2}}, \mu_{m+\frac{1}{2}} \right] \times \left[\varphi_{n-\frac{1}{2}}, \varphi_{n+\frac{1}{2}} \right],$$

where $i = 1, \dots N_x$, $j = 1, \dots N_y$, $k = 1, \dots N_w$, $m = 1, \dots N_\mu$, $n = 1, \dots N_\varphi$,

$$x_{i\pm\frac{1}{2}} = x_i \pm \frac{\Delta x_i}{2}, \quad y_{j\pm\frac{1}{2}} = y_j \pm \frac{\Delta y_j}{2},$$
$$w_{k\pm\frac{1}{2}} = w_k \pm \frac{\Delta w_k}{2}, \quad \mu_{m\pm\frac{1}{2}} = \mu_m \pm \frac{\Delta \mu_m}{2}, \quad \varphi_{n\pm\frac{1}{2}} = \varphi_n \pm \frac{\Delta \varphi_n}{2}.$$

The finite dimensional space used to approximate the functions is the space of piecewise continuous polynomials which are piecewise linear in (x, y) and piecewise constant in (w, μ, φ),

$$V_h = \{ v : v|_{\Omega_{ijkmn}} \in Q^{1,0}(\Omega_{ijkmn}) = P^1(X_{ij}) \otimes P^0(K_{kmn}) \}, \tag{3.24}$$

with the set $Q^{1,0}(\Omega_{ijkmn})$ of tensor product polynomials, linear over the element $X_{ij} = \left[x_{i-\frac{1}{2}}, x_{i+\frac{1}{2}} \right] \times \left[y_{j-\frac{1}{2}}, y_{j+\frac{1}{2}} \right]$, and constant over the element $K_{kmn} = \left[w_{k-\frac{1}{2}}, w_{k+\frac{1}{2}} \right] \times \left[\mu_{m-\frac{1}{2}}, \mu_{m+\frac{1}{2}} \right] \times \left[\varphi_{n-\frac{1}{2}}, \varphi_{n+\frac{1}{2}} \right]$.

The function Φ_h will denote the piecewise polynomial approximation of Φ over elements Ω_I,

$$\Phi_h = \sum_I \chi_I \left[T_I(t) + X_I(t)\,\frac{(x-x_i)}{\Delta x_i/2} + Y_I(t)\,\frac{(y-y_j)}{\Delta y_j/2} \right], \quad I=(i,j,k,m,n).$$

The density $\rho_h(t,x,y)$ on the cell $[x_{i-\frac{1}{2}}, x_{i+\frac{1}{2}}]\times[y_{j-\frac{1}{2}}, y_{j+\frac{1}{2}}]$ is, under this approximation,

$$\begin{aligned}
\rho_h &= \sum_{k=1}^{N_w}\sum_{m=1}^{N_\mu}\sum_{n=1}^{N_\varphi}\left[T_{ijkmn} + X_{ijkmn}\frac{(x-x_i)}{\Delta x_i/2} + Y_{ijkmn}\frac{(y-y_j)}{\Delta y_j/2}\right]\Delta w_k\Delta\mu_m\Delta\varphi_n \\
&= \sum_{k=1}^{N_w}\sum_{m=1}^{N_\mu}\sum_{n=1}^{N_\varphi} T_{ijkmn}\Delta w_k\Delta\mu_m\Delta\varphi_n \\
&+ \left(\sum_{k=1}^{N_w}\sum_{m=1}^{N_\mu}\sum_{n=1}^{N_\varphi} X_{ijkmn}\Delta w_k\Delta\mu_m\Delta\varphi_n\right)\frac{(x-x_i)}{\Delta x_i/2} \\
&+ \left(\sum_{k=1}^{N_w}\sum_{m=1}^{N_\mu}\sum_{n=1}^{N_\varphi} Y_{ijkmn}\Delta w_k\Delta\mu_m\Delta\varphi_n\right)\frac{(y-y_j)}{\Delta y_j/2}.
\end{aligned}$$

3.1. DG formulation for transformed Boltzmann equation

The Discontinuous Galerkin formulation for the Boltzmann equation (2.21) is as follows. Find $\Phi_h \in V_h$, s.t.

$$\begin{aligned}
&\int_{\Omega_{ijkmn}} (\Phi_h)_t\, v_h\, d\Omega - \int_{\Omega_{ijkmn}} g_1\Phi_h\,(v_h)_x\, d\Omega - \int_{\Omega_{ijkmn}} g_2\Phi_h\,(v_h)_y\, d\Omega \\
&+ F_x^+ - F_x^- + F_y^+ - F_y^- + F_w^+ - F_w^- + F_\mu^+ - F_\mu^- + F_\varphi^+ - F_\varphi^- \\
&= \int_{\Omega_{ijkmn}} C(\Phi_h)\, v_h\, d\Omega.
\end{aligned} \tag{3.25}$$

for any test function $v_h \in V_h$. In (3.25), the boundary integrals are given by

$$F_x^\pm = \int_{y_{j-\frac{1}{2}}}^{y_{j+\frac{1}{2}}}\int_{w_{k-\frac{1}{2}}}^{w_{k+\frac{1}{2}}}\int_{\mu_{m-\frac{1}{2}}}^{\mu_{m+\frac{1}{2}}}\int_{\varphi_{n-\frac{1}{2}}}^{\varphi_{n+\frac{1}{2}}} \widehat{g_1\Phi}\, v_h^\mp(x_{i\pm\frac{1}{2}}, y, w, \mu, \varphi)dy\,dw\,d\mu\,d\varphi,$$

$$F_y^\pm = \int_{x_{i-\frac{1}{2}}}^{x_{i+\frac{1}{2}}}\int_{w_{k-\frac{1}{2}}}^{w_{k+\frac{1}{2}}}\int_{\mu_{m-\frac{1}{2}}}^{\mu_{m+\frac{1}{2}}}\int_{\varphi_{n-\frac{1}{2}}}^{\varphi_{n+\frac{1}{2}}} \widehat{g_2\Phi}\, v_h^\mp(x, y_{j\pm\frac{1}{2}}, w, \mu, \varphi)dx\,dw\,d\mu\,d\varphi,$$

$$F_w^\pm = \int_{x_{i-\frac{1}{2}}}^{x_{i+\frac{1}{2}}}\int_{y_{j-\frac{1}{2}}}^{y_{j+\frac{1}{2}}}\int_{\mu_{m-\frac{1}{2}}}^{\mu_{m+\frac{1}{2}}}\int_{\varphi_{n-\frac{1}{2}}}^{\varphi_{n+\frac{1}{2}}} \widehat{g_3\Phi}\, v_h^\mp(x, y, w_{k\pm\frac{1}{2}}, \mu, \varphi)dx\,dy\,d\mu\,d\varphi,$$

$$F_\mu^\pm = \int_{x_{i-\frac{1}{2}}}^{x_{i+\frac{1}{2}}}\int_{y_{j-\frac{1}{2}}}^{y_{j+\frac{1}{2}}}\int_{w_{k-\frac{1}{2}}}^{w_{k+\frac{1}{2}}}\int_{\varphi_{n-\frac{1}{2}}}^{\varphi_{n+\frac{1}{2}}} \widehat{g_4\Phi}\, v_h^\mp(x, y, w, \mu_{m\pm\frac{1}{2}}, \varphi)dx\,dy\,dw\,d\varphi,$$

$$F_\varphi^\pm = \int_{x_{i-\frac{1}{2}}}^{x_{i+\frac{1}{2}}}\int_{y_{j-\frac{1}{2}}}^{y_{j+\frac{1}{2}}}\int_{w_{k-\frac{1}{2}}}^{w_{k+\frac{1}{2}}}\int_{\mu_{m-\frac{1}{2}}}^{\mu_{m+\frac{1}{2}}} \widehat{g_5\Phi}\, v_h^\mp(x, y, w, \mu, \varphi_{n\pm\frac{1}{2}})dx\,dy\,dw\,d\mu,$$

where the upwind numerical fluxes $\widehat{g_s\Phi}$, $s=1,\ldots,5$ are defined as

$$\widehat{g_1\Phi}|_{x_{i\pm1/2}} = \left(\frac{g_1+|g_1|}{2}\right)\Phi_h|^-_{x_{i\pm1/2}} + \left(\frac{g_1-|g_1|}{2}\right)\Phi_h|^+_{x_{i\pm1/2}},$$
$$\widehat{g_2\Phi}|_{y_{j\pm1/2}} = \left(\frac{g_2+|g_2|}{2}\right)\Phi_h|^-_{y_{j\pm1/2}} + \left(\frac{g_2-|g_2|}{2}\right)\Phi_h|^+_{y_{j\pm1/2}},$$
$$\widehat{g_3\Phi}|_{w_{k\pm1/2}} = \left(\frac{g_3+|g_3|}{2}\right)\Phi_h|^-_{w_{k\pm1/2}} + \left(\frac{g_3-|g_3|}{2}\right)\Phi_h|^+_{w_{k\pm1/2}},$$
$$\widehat{g_4\Phi}|_{\mu_{m\pm1/2}} = \left(\frac{g_4+|g_4|}{2}\right)\Phi_h|^-_{\mu_{m\pm1/2}} + \left(\frac{g_4-|g_4|}{2}\right)\Phi_h|^+_{\mu_{m\pm1/2}},$$
$$\widehat{g_5\Phi}|_{\varphi_{n\pm1/2}} = \left(\frac{g_5+|g_5|}{2}\right)\Phi_h|^-_{\varphi_{n\pm1/2}} + \left(\frac{g_5-|g_5|}{2}\right)\Phi_h|^+_{\varphi_{n\pm1/2}}. \tag{3.26}$$

3.2. Poisson equation – local discontinuous Galerkin (LDG) Method

The Poisson equation (2.23) is solved by the LDG method as in [29].

By means of this scheme we find a solution $\Psi_h, q_h, s_h \in W_h^1$, where $(q,s) = (\partial_x\Psi, \partial_y\Psi)$ and $W_h^1 = \{v : v|_{X_{ij}} \in P^1(X_{ij})\}$, $P^1(X_{ij})$ the set of linear polynomials on X_{ij}. It involves rewriting the equation into the form

$$\begin{cases} q = \dfrac{\partial\Psi}{\partial x}, \qquad s = \dfrac{\partial\Psi}{\partial y}, \\ \dfrac{\partial}{\partial x}(\epsilon_r q) + \dfrac{\partial}{\partial y}(\epsilon_r s) = R(t,x,y), \end{cases} \tag{3.27}$$

where $R(t,x,y) = c_p[\rho(t,x,y) - \mathcal{N}_D(x,y)]$ is a known function that can be computed at each time step once Φ is solved from (3.25), and the coefficient ϵ_r depends on x, y. The Poisson system is only on the (x,y) domain. Hence, we use the grid $I_{ij} = \left[x_{i-\frac12}, x_{i+\frac12}\right] \times \left[y_{j-\frac12}, y_{j+\frac12}\right]$, with $i = 1,\dots,N_x$, $j = 1,\dots,N_y+M_y$, where $j = N_y+1,\dots,N_y+M_y$ denotes the oxide-silicon region, and the grid in $j = 1,\dots,N_y$ is consistent with the five-dimensional rectangular grid for the Boltzmann equation in the silicon region. The approximation space is defined as

$$W_h^\ell = \{v : v|_{I_{ij}} \in P^\ell(I_{ij})\}. \tag{3.28}$$

Here $P^\ell(I_{ij})$ denotes the set of all polynomials of degree at most ℓ on I_{ij}. The LDG scheme for (3.27) is: to find $q_h, s_h, \Psi_h \in V_h^\ell$, such that

$$0 = \int_{I_{ij}} [q_h v_h + \Psi_h (v_h)_x]\,dxdy + \int_{y_{j-\frac12}}^{y_{j+\frac12}} \left[\hat\Psi_h v_h^+\Big|(x_{i-\frac12},y) - \hat\Psi_h v_h^-\Big|(x_{i+\frac12},y)\right]dy,$$

$$0 = \int_{I_{ij}} \left[s_h w_h + \Psi_h (w_h)_y\right]dxdy + \int_{x_{i-\frac12}}^{x_{i+\frac12}} \left[\tilde\Psi_h w_h^+\Big|(x,y_{j-\frac12}) - \tilde\Psi_h w_h^-\Big|(x,y_{j+\frac12})\right]dx,$$

$$- \int_{I_{i,j}} \epsilon_r q_h (p_h)_x dxdy + \int_{y_{j-\frac12}}^{y_{j+\frac12}} \widehat{\epsilon_r q_h} p_h^-(x_{i+\frac12},y)dy - \int_{y_{j-\frac12}}^{y_{j+\frac12}} \widehat{\epsilon_r q_h} p_h^+(x_{i-\frac12},y)dy$$

$$- \int_{I_{i,j}} \epsilon_r s_h (p_h)_y dxdy + \int_{x_{i-\frac12}}^{x_{i+\frac12}} \widetilde{\epsilon_r s_h} p_h^-(x,y_{j+\frac12})dx - \int_{x_{i-\frac12}}^{x_{i+\frac12}} \widetilde{\epsilon_r s_h} p_h^+(x,y_{j-\frac12})dx$$

$$= \int_{I_{i,j}} R(t,x,y) p_h dxdy, \tag{3.29}$$

hold true for any $v_h, w_h, p_h \in W_h^\ell$. In the above formulation, we choose the flux as follows, in the x-direction, we use $\hat\Psi_h = \Psi_h^-$, $\widehat{\epsilon_r q_h} = \epsilon_r q_h^+ - [\Psi_h]$. In the y-direction, we use $\tilde\Psi_h = \Psi_h^-$, $\widetilde{\epsilon_r s_h} = \epsilon_r s_h^+ - [\Psi_h]$. On some part of the domain boundary, the above flux needs to be changed to accommodate various boundary conditions. For example, in the case of a double gate

MOSFET device, for the boundary condition of the Poisson equation, $\Psi = \Psi_S$ at source, $\Psi = \Psi_D$ at drain and $\Psi = \Psi_G$ at gate. For the rest of the boundary regions, we have homogeneous Neumann boundary conditions, i.e., $\frac{\partial \Psi}{\partial n} = 0$. The relative dielectric constant in the oxide-silicon region is $\epsilon_r = 3.9$, in the silicon region is $\epsilon_r = 11.7$. Near the drain then, we are given Dirichlet boundary condition, so we need to flip the flux in x-direction: let $\hat{\Psi}_h(x_{i+\frac{1}{2}}, y) = \Psi_h^+(x_{i+\frac{1}{2}}, y)$ and $\widehat{\epsilon_r q_h}(x_{i+\frac{1}{2}}, y) = \epsilon_r q_h^-(x_{i+\frac{1}{2}}, y) - [\Psi_h](x_{i+\frac{1}{2}}, y)$, if the point $(x_{i+\frac{1}{2}}, y)$ is at the drain. For the gate, we need to flip the flux in y-direction: let $\tilde{\Psi}_h(x, y_{j+\frac{1}{2}}) = \Psi_h^+(x, y_{j+\frac{1}{2}})$ and $\widetilde{\epsilon_r s_h}(x, y_{j+\frac{1}{2}}) = \epsilon_r s_h^-(x, y_{j+\frac{1}{2}}) - [\Psi_h](x, y_{j+\frac{1}{2}})$, if the point $(x, y_{j+\frac{1}{2}})$ is at the gate. For the bottom, we need to use the Neumann condition, and flip the flux in y-direction, i.e., $\tilde{\Psi}_h = \Psi_h^+$, $\widetilde{\epsilon_r s_h} = \epsilon_r s_h^-$. This scheme described above will enforce the continuity of Ψ and $\epsilon_r \frac{\partial \Psi}{\partial n}$ across the interface of silicon and oxide-silicon interface. The solution of (3.29) gives us approximations to both the potential Ψ_h and the electric field $(E_x)_h = -c_v q_h$, $(E_y)_h = -c_v s_h$.

3.3. RK-DG algorithm for BP, from t^n to t^{n+1}

The following RK-DG algorithm for BP is a dynamic extension of the Gummel iteration map. We write below the steps to evolve from time t^n to time t^{n+1}.

1. Compute the electron density $\rho_h(x, y, t)$.
2. Solve Poisson Eq. for the given $\rho_h(x, y, t)$ by Local DG, obtaining the potential Ψ_h and the electric field $\mathbf{E}_h = -(q_h, s_h)$. Compute then the respective transport terms g_s, $s = 1, ..., 5$.
3. Solve by DG the advection and collision part of the Boltzmann Equation. A Method of Lines (an ODE system) for the time dependent coefficients of Φ_h (degrees of freedom) is obtained.
4. Evolve ODE system by Runge–Kutta from t^n to t^{n+1}. (If partial time step necessary, repeat Step 1 to 3 as needed).

4. Boundary conditions implementation for 2D-$\vec{x}$, 3D-$\vec{k}$ devices at x, w, μ, φ boundaries

We will consider in this work 2D devices in position space, which need a 3D momentum description for kinetic equations modeling semiconductors. For example, a common device of interest is a 2D double gate MOSFET. A schematic plot of it is given in Fig. 4.1. The shadowed region denotes the oxide-silicon region, whereas the rest is the silicon region. Potential bias are applied at the source, drain, and gates. The problem is symmetric about the x-axis.

Another possible 2D problem is the case of a bi-dimensional bulk silicon diode, for which the doping is constant all over the physical domain, and which would have just an applied potential (bias) between the source $x = 0$ and the drain $x = L_x$ (no gates), with insulating reflecting boundaries at $y = 0$ and $y = L_y$.

We consider in the following sections the different kinds of boundary conditions for 2D devices and their numerical implementation, either at $\vec{x}$-boundaries or at $\vec{w}$-boundaries.

4.1. Poisson equation boundary condition

The BC for Poisson Eq. are imposed over the (x, y)-domain.

For example, for the case of a 2D Double gated MOSFET, Dirichlet BC would be imposed to the potential Ψ, as we have three different applied potentials biases, $\Psi = 0.5235$ Volts at the source $x = 0$, $\Psi = 1.5235$ Volts at the drain $x = L_x$, $\Psi = 1.06$ Volts at the gates. Homogeneous Neumann BC would be imposed for the rest of the boundaries, that is, $\partial_{\hat{n}} \Psi = 0$.

For the case of a 2D bulk silicon diode, we impose Dirichlet BC for the difference of potential Ψ between source and drain, $\Psi = 0.5235$ Volts at the source $x = 0$, $\Psi = 1.5235$ Volts at the drain $x = L_x$. For the boundaries $y = 0$, L_y we impose Homogeneous Neumann BC too, that is, $\partial_y \Psi|_{y_0} = 0$, $y_0 = 0$, L_y.

4.2. Charge neutrality BC

As in [29], at the source and drain contacts, we implement the charge neutrality boundary condition (1.7). Ghost cells for $i = 0$ and $i = N_x + 1$ at the respective boundaries are used, implementing numerically the boundary conditions

$$\Phi(i = 0) = \Phi(i = 1) \frac{N_D(i = 1)}{\rho(i = 1)},$$
$$\Phi(i = N_x + 1) = \Phi(i = N_x) \frac{N_D(i = N_x)}{\rho(i = N_x)}.$$

4.3. Cut-off BC

In the (w, μ, φ)-space, we only need to apply a cut-off Boundary Condition. At $w = w_{\max}$, Φ_h is made machine zero,

$$\Phi_h(x, y, w, \mu, \varphi, t)|_{w = w_{\max}} = 0. \tag{4.30}$$

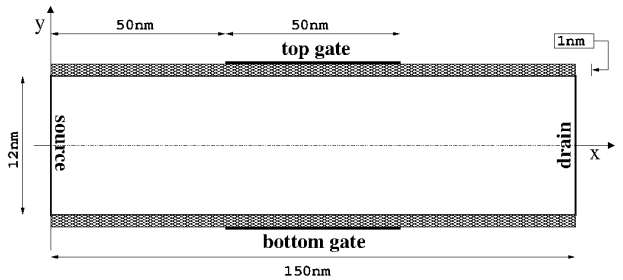

Fig. 4.1. Schematic representation of a 2D double gate MOSFET device. From Y. Cheng, I. M. Gamba, A. Majorana and C.-W. Shu, 'A discontinuous Galerkin solver for Boltzmann Poisson systems in nano devices', Computer Methods in Applied Mechanics and Engineering, v198 (2009), p. 3143.

No other boundary condition is necessary for $\vec{w}$-boundaries, since analytically we have that

- at $w = 0$, $g_3 = 0$,
- at $\mu = \pm 1$, $g_4 = 0$,
- at $\varphi = 0, \pi$, $g_5 = 0$,

so, at such regions, the numerical flux always vanishes.

5. Reflection BC on BP

Reflection Boundary Conditions can be expressed in the form

$$f(\vec{x}, \vec{k}, t)|_{\Gamma_{N^-}} = F_R(f|_{\Gamma_{N^+}}), \tag{5.31}$$

such that the following pointwise zero flux condition is satisfied at reflecting boundaries, so

$$0 = \eta(\vec{x}) \cdot J(\vec{x}, t) = \eta(\vec{x}) \cdot \int_{\Omega_{\vec{k}}} \vec{v}(\vec{k})\, f(\vec{x}, \vec{k}, t)\, d\vec{k}, \tag{5.32}$$

$$0 = \int_{\eta\cdot\vec{v}>0} \eta(\vec{x}) \cdot \vec{v}(\vec{k})\, f(\vec{x}, \vec{k}, t)|_{\Gamma_{N^+}}\, d\vec{k} + \int_{\eta\cdot\vec{v}<0} \eta(\vec{x}) \cdot \vec{v}(\vec{k})\, f(\vec{x}, \vec{k}, t)|_{\Gamma_{N^-}}\, d\vec{k},$$

$$0 = \int_{\vec{v}\cdot\eta>0} \vec{v} \cdot \eta\, f|_{\Gamma_{N^+}}\, d\vec{k} + \int_{\vec{v}\cdot\eta<0} \vec{v} \cdot \eta\, F_R(f|_{\Gamma_{N^+}})\, d\vec{k},$$

as in Cercignani, Gamba, Levermore [4], where the given BC at Neumann boundary regions at the kinetic level is such that the particle flow vanishes.

For simplicity we write $\vec{v} = \vec{v}(\vec{k}) = \nabla_{\vec{k}}\varepsilon(\vec{k})/\hbar$. We will study three kinds of reflective boundary conditions: specular, diffusive, and mixed reflection. The last one is a convex combination of the previous two, but the convexity parameter can be either constant or momentum dependant, $p(\vec{k})$. We go over the mathematics and numerics related to these conditions below.

5.1. Specular reflection

It is clear that, at the analytical level, the specular reflection BC (1.12) satisfies the zero flux condition pointwise at reflecting boundaries, since

$$\int_{\eta\cdot\vec{v}>0} |\eta(\vec{x}) \cdot \vec{v}(\vec{k})|\, f(\vec{x}, \vec{k}, t)\Big|_{\Gamma_{N^+}} d\vec{k} - \int_{-\eta\cdot\vec{v}<0} |\eta(\vec{x}) \cdot \vec{v}(\vec{k})|\, f(\vec{x}, \vec{k}', t)\Big|_{\Gamma_{N^+}} d\vec{k} = 0.$$

Specular reflection BC in our transformed Boltzmann Eq. for the new coordinate system is mathematically formulated in our problem as

$$\Phi|_-(x, y, w, \mu, \varphi, t) = \Phi|_+(x, y, w, \mu, \pi - \varphi, t), \quad (x, y, w, \mu, \varphi) \in \Gamma_N^-. \tag{5.33}$$

To impose numerically specular reflection BC at $y = 0, L_y$ in the DG method, we follow the procedure of [29]. We relate the inflow values of the pdf, associated to the outer ghost cells, to the outflow values of the pdf, which are associated to the interior cells adjacent to the boundary, as given below by

$$\Phi_h|_-(x, y_{1/2}, w, \mu, \varphi, t) = \Phi_h|_+(x, y_{1/2}, w, \mu, \pi - \varphi, t), \quad y_{1/2} = 0, \tag{5.34}$$
$$\Phi_h|_-(x, y_{N_y+\frac{1}{2}}, w, \mu, \varphi, t) = \Phi_h|_+(x, y_{N_y+\frac{1}{2}}, w, \mu, \pi - \varphi, t), \quad y_{N_y+\frac{1}{2}} = L_y.$$

In the case of the boundary $y_{1/2} = 0$, assuming $\Delta y_0 = \Delta y_1$, $\Delta\varphi_{n'} = \Delta\varphi_n$, with $n' = N_\varphi - n + 1$, if $(x, y_{1/2} - y, w, \mu, \varphi) \in \Omega_{i0kmn}$ then $(x, y_{1/2} + y, w, \mu, \pi - \varphi) \in \Omega_{i1kmn'}$. The values of $\Phi_h|^{\pm}_{y_{1/2}}$ at the related inner and outer boundary cells Ω_{i0kmn} ($j = 0$) and $\Omega_{i1kmn'}$ ($j = 1$) must be equal at the boundary $y_{1/2} = 0$. Indeed

$$\Phi_h|^-_{\Omega_{i0kmn}}(x, y_{1/2}, w, \mu, \varphi, t) = \Phi_h|^+_{\Omega_{i1kmn'}}(x, y_{1/2}, w, \mu, \pi - \varphi, t) \Longrightarrow$$
$$T_{i0kmn} + X_{i0kmn}\frac{(x - x_i)}{\Delta x_i/2} + Y_{i0kmn}\frac{(y_{1/2} - y_0)}{\Delta y_0/2} =$$
$$T_{i1kmn'} + X_{i1kmn'}\frac{(x - x_i)}{\Delta x_i/2} + Y_{i1kmn'}\frac{(y_{1/2} - y_1)}{\Delta y_1/2}.$$

Therefore, from the equality above we find the relation between the coefficients of Φ_h at inner and outer adjacent boundary cells, given by

$$T_{i0kmn} = T_{i1kmn'},\ X_{i0kmn} = X_{i1kmn'},\ Y_{i0kmn} = -Y_{i1kmn'}. \tag{5.35}$$

Following an analogous procedure for the boundary $y_{N_y+1/2}$, we have

$$\Phi_h|^-_{\Omega_{i,N_y+1,kmn}}(x, y_{N_y+\frac{1}{2}}, w, \mu, \varphi, t) = \Phi_h|^+_{\Omega_{i,N_y,kmn'}}(x, y_{N_y+\frac{1}{2}}, w, \mu, \pi - \varphi, t).$$

Then

$$T_{i,N_y+1,kmn} + X_{i,N_y+1,kmn}\frac{(x - x_i)}{\Delta x_i/2} + Y_{i,N_y+1,kmn}\frac{(y_{N_y+\frac{1}{2}} - y_{N_y+1})}{\Delta y_{N_y+1}/2} =$$
$$T_{i,N_y,kmn'} + X_{i,N_y,kmn'}\frac{(x - x_i)}{\Delta x_i/2} + Y_{i,N_y,kmn'}\frac{(y_{N_y+\frac{1}{2}} - y_{N_y})}{\Delta y_{N_y}/2}, \tag{5.36}$$

and hence

$$T_{i,N_y+1,kmn} = T_{i,N_y,kmn'},\ X_{i,N_y+1,kmn} = X_{i,N_y,kmn'},\ Y_{i,N_y+1,kmn} = -Y_{i,N_y,kmn'}.$$

5.2. Diffusive reflection

The diffusive reflection BC can be formulated as

$$f(\vec{x}, \vec{k}, t)|_- = F_D(f|_+) = C\,\sigma\{f|_+\}(\vec{x}, t)\, e^{-\varepsilon(\vec{k})/K_B T_L}, \quad (\vec{x}, \vec{k}) \in \Gamma_N^-, \tag{5.37}$$

where $\sigma\{f|_+\}(\vec{x}, t) = \sigma(\vec{x}, t)$ and $C = C\{\eta(\vec{x})\}$ are the function and parameter such that the zero flux condition is satisfied at each of the points of the Neumann Boundary, so

$$0 = \int_{\vec{v}\cdot\eta>0} \vec{v}\cdot\eta\, f|_{\Gamma_{N^+}}\, d\vec{k} + \int_{\vec{v}\cdot\eta<0} \vec{v}\cdot\eta \left[C\sigma(\vec{x}, t) e^{-\varepsilon(\vec{k})/K_B T_L}\right] d\vec{k},$$
$$0 = \int_{\vec{v}\cdot\eta>0} \vec{v}\cdot\eta\, f|_{\Gamma_{N^+}}\, d\vec{k} - \sigma(\vec{x}, t)\cdot C \int_{\vec{v}\cdot\eta<0} |\vec{v}\cdot\eta|\, e^{-\varepsilon(\vec{k})/K_B T_L}\, d\vec{k}.$$

It follows then that

$$\sigma\{f|_+\}(\vec{x}, t) = \int_{\vec{v}(\vec{k})\cdot\eta>0} \vec{v}\cdot\eta\, f|_{\Gamma_{N^+}}(\vec{x}, \vec{k}, t)\, d\vec{k}, \tag{5.38}$$

$$C\left\{\eta(\vec{x})\right\} = \left(\int_{\vec{v}\cdot\eta<0} |\vec{v}\cdot\eta|\, e^{-\varepsilon(\vec{k})/K_B T_L}\, d\vec{k}\right)^{-1}, \tag{5.39}$$

$$f(\vec{x}, \vec{k}, t)|_- = \frac{e^{-\varepsilon(\vec{k})/K_B T_L} \int_{\vec{v}(\vec{k})\cdot\eta>0} \vec{v}\cdot\eta\, f|_{\Gamma_{N^+}}(\vec{x}, \vec{k}, t)\, d\vec{k}}{\int_{\vec{v}\cdot\eta<0} |\vec{v}\cdot\eta|\, e^{-\varepsilon(\vec{k})/K_B T_L}\, d\vec{k}}. \tag{5.40}$$

The diffusive reflection BC, formulated in terms of the unknown function Φ of the transformed Boltzmann Equation (2.21), is expressed as

$$\Phi|_-(x,y,w,\mu,\varphi,t) = F_D(\Phi|_+) = C\,\sigma\left\{\Phi|_+\right\}(x,y,t)\,e^{-w}s(w)\,, \tag{5.41}$$

$$\sigma(x,y,t) = \int\limits_{(g_1,g_2)\cdot\eta>0} \eta\cdot(g_1,g_2)(w,\mu,\varphi)\,\Phi|_+\,dwd\mu d\varphi\,, \tag{5.42}$$

$$C(\eta) = \left(\int\limits_{(g_1,g_2)\cdot\eta<0} |(g_1,g_2)\cdot\eta|\,e^{-w}s(w)\,dwd\mu d\varphi\right)^{-1}. \tag{5.43}$$

We have, over the portion of the boundary considered, that $\eta=(0,-1,0)$ for $y=0$ and $\eta=(0,1,0)$ for $y=L_y$. Therefore

$$\Phi|_-(x,y_b,w,t) = \frac{e^{-w}s(w)\int_{-g_2>0}|g_2|\,\Phi|_+\,dwd\mu d\varphi}{\int_{-g_2<0}|g_2|\,e^{-w}s(w)\,dwd\mu d\varphi}\,,\quad y_b=0\,, \tag{5.44}$$

$$\Phi|_-(x,y_b,w,t) = \frac{e^{-w}s(w)\int_{+g_2>0}|g_2|\,\Phi|_+\,dwd\mu d\varphi}{\int_{+g_2<0}|g_2|\,e^{-w}s(w)\,dwd\mu d\varphi}\,,\quad y_b=L_y\,. \tag{5.45}$$

5.2.1. Numerical formulation of diffusive BC for DG

For the DG numerical method, we have to project the boundary conditions to be imposed in the space V_h. Our goal is to have at the numerical level an equivalent pointwise zero flux condition at the reflection boundary regions.

We formulate then the diffusive BC for the DG method as

$$\begin{aligned}\Phi_h|_-(x,y_b,w,\mu,\varphi,t) &= \Pi_h\left\{F_D(\Phi_h|_+)\right\}\\ &= \Pi_h\left\{C\,\sigma_h\left\{\Phi_h|_+\right\}(x,y_b,t)\,e^{-w}s(w)\right\},\quad y_b=0,L_y,\end{aligned}$$

where Π_h is the projector of functions into the finite element space V_h, $\sigma_h\in V_h$ is a function in our piecewise polynomial space for (x,y) and C is a parameter such that the zero flux condition is satisfied numerically, so

$$\begin{aligned}0 &= \int\limits_{\vec{g}\cdot\eta>0}\vec{g}\cdot\eta\,\Phi_h|_+d\vec{w} + \int\limits_{\vec{g}\cdot\eta<0}\vec{g}\cdot\eta\,\Phi_h|_-d\vec{w}\\ &= \int\limits_{\vec{g}\cdot\eta>0}\vec{g}\cdot\eta\,\Phi_h|_+d\vec{w} + \int\limits_{\vec{g}\cdot\eta<0}\vec{g}\cdot\eta\,\Pi_h\left\{F_D(\Phi_h|_+)\right\}d\vec{w}\\ &= \int\limits_{\vec{g}\cdot\eta>0}\vec{g}\cdot\eta\,\Phi_h|_+d\vec{w} + \int\limits_{\vec{g}\cdot\eta<0}\vec{g}\cdot\eta\,\Pi_h\left\{C\,\sigma_h\left\{\Phi_h|_+\right\}(x,y_b,t)\,e^{-w}s(w)\right\}d\vec{w}\,.\end{aligned} \tag{5.46}$$

In the space V_h of piecewise continuous polynomials which are tensor products of polynomials of degree p in $\vec{x}$ and of degree q in $\vec{w}$, it holds that

$$\Pi_h\left\{f_1(\vec{x})f_2(\vec{w})\right\} = \Pi_h\left\{f_1(\vec{x})\right\}\,\Pi_h\left\{f_2(\vec{w})\right\}\,, \tag{5.47}$$

$$V_h = \{v : v|_{\Omega_{ijkmn}}\in Q^{p,q}(\Omega_{ijkmn}) = P^p(X_{ij})\otimes P^q(K_{kmn})\}.$$

Therefore, for our particular case we have

$$\Pi_h\left\{C\,\sigma_h(x,y_b,t)\,e^{-w}s(w)\right\} = C\,\sigma_h(x,y_b,t)\,\Pi_h\left\{e^{-w}s(w)\right\}\,, \tag{5.48}$$

so for the numerical zero flux condition pointwise we have that

$$\begin{aligned}0 &= \int\limits_{\vec{g}\cdot\eta>0}\vec{g}\cdot\eta\,\Phi_h|_+d\vec{w} + \int\limits_{\vec{g}\cdot\eta<0}\vec{g}\cdot\eta\,C\,\sigma_h\left\{\Phi_h|_+\right\}(x,y_b,t)\,\Pi_h\left\{e^{-w}s(w)\right\}d\vec{w}\\ 0 &= \int\limits_{\vec{g}\cdot\eta>0}\vec{g}\cdot\eta\,\Phi_h|_+d\vec{w} - \sigma_h\left\{\Phi_h|_+\right\}(x,y_b,t)\,C\int\limits_{\vec{g}\cdot\eta<0}|\vec{g}\cdot\eta|\,\Pi_h\left\{e^{-w}s(w)\right\}d\vec{w}\,.\end{aligned}$$

We observe then that we can obtain a numerical equivalent of the pointwise zero flux condition if we define

$$C\{\eta\} = C\left\{\pm\hat{y}\right\} = \left(\int\limits_{\pm g_2 = \vec{g}\cdot\eta < 0} |\vec{g}\cdot\eta|\, \Pi_h\left\{e^{-w} s(w)\right\} d\vec{w} \right)^{-1}, \quad \eta = \pm\hat{y}\,.$$

$$\sigma_h\{\Phi_h|_+\}(x, y_b, t) = \int\limits_{\pm\hat{y}\cdot\vec{g}>0} \vec{g}\cdot\eta\, \Phi_h|_+ d\vec{w} = \sigma\{\Phi_h|_+\}(x, y_b, t)\,,\ y_b = 0,\ L_y\,.$$

In our particular case, in which we have chosen our function space as piecewise linear in (x, y) and piecewise constant in (w, μ, φ), the projection of the Maxwellian is a piecewise constant approximation representing its average value over each momentum cell, that is

$$\Pi_h\left\{e^{-w} s(w)\right\} = \sum_{k,m,n} \chi_{kmn} \frac{\int_{kmn} e^{-w} s(w) dw d\mu d\varphi}{\Delta w_k \Delta\mu_m \Delta\varphi_n} = \sum_{k,m,n} \chi_{kmn} \frac{\int_{w_{k-}}^{w_{k+}} e^{-w} s(w) dw}{\Delta w_k}.$$

Therefore, for the particular space we have chosen, we have that

$$\sigma_h\{\Phi_h|_+\}(x, y_b, t) = \int\limits_{\pm g_2>0} \pm g_2\, \Phi_h|_+ d\vec{w} = \sigma\{\Phi_h|_+\}(x, y_b, t)\,, \tag{5.49}$$

$$y_b = 0 = y_{1/2} \quad (\eta = -\hat{y})\,, \quad \text{or} \quad y_b = L_y = y_{N_y+1/2} \quad (\eta = +\hat{y})\,,$$

$$C^{-1} = \sum_{k,m,n}^{\pm g_2<0} \frac{1}{\Delta w_k} \int_{w_{k-1/2}}^{w_{k+1/2}} e^{-w} s(w)\, dw \int\limits_{k,m,n} |g_2|\, dw\, d\mu\, d\varphi, \quad \eta = \pm\hat{y}\,,$$

$$\Phi_h|_-(x, y_b, w, \mu, \varphi, t) = C\,\sigma_h\{\Phi_h|_+\}(x, y_b, t)\,\Pi_h\left\{e^{-w} s(w)\right\}, \quad y_b = 0,\ L_y,$$

$$\Phi_h|_-(x, y_b, w, \mu, \varphi, t) = \frac{\int_{\pm g_2>0} |g_2|\, \Phi_h|_+ d\vec{w} \ \sum_{k,m,n}^{\pm g_2<0} \chi_{kmn} \frac{\int_k e^{-w} s(w)\, dw}{\Delta w_k}}{\sum_{k,m,n}^{\pm g_2<0} \int_{kmn} |g_2|\, dw\, d\mu\, d\varphi\, \frac{\int_k e^{-w} s(w)\, dw}{\Delta w_k}}\,.$$

By the upper index $\pm g_2 < 0$ in a sum we mean to say that the sum is taken over the values of k, m, n for which $\pm g_2 = \vec{g}\cdot\eta < 0$. We notice that the polynomial approximation σ_h is equal to the analytical function σ operating on the polynomial approximation $\Phi_h|_+$. However, the constant C needed in order to achieve the zero flux condition numerically is not equal to the value of this parameter in the analytical solution. In this case C is an approximation of the analytical value using a piecewise constant approximation of the Maxwellian (its average over cells).

The approximate operator $\sigma_h\{\Phi_h|_+\}(x, y, t)$ gives a piecewise linear polynomial dependant on (x, y) with time dependent coefficients. We have that

$$\Phi_h|_+ \in V_h \Longrightarrow \sigma_h\{\Phi_h|_+\}(x, y, t) = \int\limits_{\pm\cos\varphi>0} |g_2|\, \Phi_h|_+ dw d\mu d\varphi \in V_h\,,$$

where $\Phi_h|_+$ is such that, at the boundary $y = y_b$ of the cell Ω_{ijkmn}, it is given by

$$\Phi_h|_+(t, x, y, w, \mu, \varphi) = T_{ijkmn}(t) + X_{ijkmn}(t)\,\frac{2(x - x_i)}{\Delta x_i} + Y_{ijkmn}(t)\,\frac{2(y - y_j)}{\Delta y_j}\,.$$

We define $I = ijkmn$, so in $\Omega_I = X_{ij} \times K_{kmn}$. Then,

$$\sigma_h(x, y, t) = \sigma_I^0(t) + \sigma_I^x(t)\frac{(x - x_i)}{\Delta x_i/2} + \sigma_I^y(t)\frac{(y - y_j)}{\Delta y_j/2}\,. \tag{5.50}$$

We summarize the main results of these calculations for σ_h and $\Phi_h|_-$, by showing just the ones related to $y = L_y$ (the case $y = 0$ is analogous). At the boundary $y = L_y$, the inner cells associated to outflow have $j = N_y$, adjacent to the boundary, whereas the ghost cells related to inflow have the index $j = N_y + 1$. We compute the integral σ_h as

$$\sigma_h\{\Phi_h|_+\}(x, y, t) = \int\limits_{\cos\varphi\geq 0} \frac{\sqrt{w(1 + \alpha_K w)}}{1 + 2\alpha_K w}\sqrt{1 - \mu^2}\cos\varphi\ \Phi_h|_+ dw d\mu d\varphi$$

$$= \sum_{k,m,n}^{n\leq\frac{N_p}{2}} \int\limits_{K_{kmn}} \frac{\sqrt{w(1 + \alpha_K w)}}{1 + 2\alpha_K w}\sqrt{1 - \mu^2}\cos\varphi\, \Phi_h|_+ dw d\mu d\varphi.$$

Therefore, we have, with $I = (i, j, k, m, n)$, $j = N_y$ below, that

$$\sigma_I^0 = \sum_{k,m,n}^{n \le \frac{N_\varphi}{2}} T_{iN_ykmn} \int_{w_{k-1/2}}^{w_{k+1/2}} \frac{\sqrt{w(1+\alpha_K w)}}{1+2\alpha_K w} dw \int_{\mu_{m-1/2}}^{\mu_{m+1/2}} \sqrt{1-\mu^2} d\mu \int_{\varphi_{n-1/2}}^{\varphi_{n+1/2}} \cos\varphi d\varphi,$$

$$\sigma_I^x = \sum_{k,m,n}^{n \le \frac{N_\varphi}{2}} X_{iN_ykmn} \int_{w_{k-1/2}}^{w_{k+1/2}} \frac{\sqrt{w(1+\alpha_K w)}}{1+2\alpha_K w} dw \int_{\mu_{m-1/2}}^{\mu_{m+1/2}} \sqrt{1-\mu^2} d\mu \int_{\varphi_{n-1/2}}^{\varphi_{n+1/2}} \cos\varphi d\varphi,$$

$$\sigma_I^y = \sum_{k,m,n}^{n \le \frac{N_\varphi}{2}} Y_{iN_ykmn} \int_{w_{k-1/2}}^{w_{k+1/2}} \frac{\sqrt{w(1+\alpha_K w)}}{1+2\alpha_K w} dw \int_{\mu_{m-1/2}}^{\mu_{m+1/2}} \sqrt{1-\mu^2} d\mu \int_{\varphi_{n-1/2}}^{\varphi_{n+1/2}} \cos\varphi d\varphi.$$

Once the coefficients of σ_h have been computed, we use them to obtain the polynomial approximation $\Phi_h|_-$, with $j = N_y + 1$, from (5.49)

$$\Phi_h|_{y=L_y}^- = \sum_i \sum_{k,m,n}^{n \ge \frac{N_\varphi}{2}} \chi_{iN_ykmn} C \left[\sigma_I^0 + \sigma_I^x \frac{(x-x_i)}{\Delta x_i/2} + \sigma_I^y \cdot 1 \right] \frac{\int_k e^{-w} s(w) dw}{\Delta w_k}.$$

We have at the same time, by definition, that

$$\Phi_h|_{y=L_y}^- = \sum_{ikmn}^{n \ge \frac{N_\varphi}{2}} \chi_{i,N_y+1,kmn} \left[T_{i,N_y+1,k,m,n} + X_{i,N_y+1,k,m,n} \frac{(x-x_i)}{\Delta x_i/2} - 1 \cdot Y_{i,N_y+1,k,m,n} \right].$$

Therefore, the coefficients for $\Phi_h|_{y=L_y}^-$ are

$$T_{i,N_y+1,kmn}(t) = C\sigma^0_{iN_ykmn}(t) \frac{\int_k e^{-w} s(w) dw}{\Delta w_k}, \tag{5.51}$$

$$X_{i,N_y+1,kmn}(t) = C\sigma^x_{iN_ykmn}(t) \frac{\int_k e^{-w} s(w) dw}{\Delta w_k}, \tag{5.52}$$

$$Y_{i,N_y+1,kmn}(t) = -1 \cdot C\sigma^y_{iN_ykmn}(t) \frac{\int_k e^{-w} s(w) dw}{\Delta w_k}, \tag{5.53}$$

keeping in mind that our parameter C is given by the formula

$$C^{-1} = \sum_{kmn}^{n \ge \frac{N_p}{2}} \frac{\int_k e^{-w} s(w) dw}{\Delta w_k} \int_k \frac{\sqrt{w(1+\alpha_K w)}}{1+2\alpha_K w} dw \int_m \sqrt{1-\mu^2} d\mu \int_n \cos\varphi d\varphi.$$

5.3. Mixed reflection

The mixed reflection condition is a convex combination of the specular and diffusive reflections:

$$f(\vec{x}, \vec{k}, t)|_- = p f|_+(\vec{x}, \vec{k}', t) + (1-p) C\sigma \{f|_+\}(\vec{x}, t) e^{-\varepsilon(\vec{k})/K_B T}, \quad (\vec{x}, \vec{k}) \in \Gamma_N^-,$$

p is the Specularity Parameter, $0 \le p \le 1$. p can be either constant or $p = p(\vec{k})$, a function of the wave vector momentum.

For p constant, it can be shown easily that the previous formulas obtained for the specular and diffusive BC, in particular the previous formulas for $\sigma\ C(x)$, works also in this case to obtain a zero flux condition at the Neumann boundaries:

$$\begin{aligned}
\eta \cdot J &= \int_{\vec{v}\cdot\eta>0} \vec{v} \cdot \eta f|_+ d\vec{k} + \int_{\vec{v}\cdot\eta<0} \vec{v} \cdot \eta \left[p f(\vec{x}, \vec{k}', t)|_+ + (1-p) C e^{\frac{-\varepsilon(\vec{k})}{K_B T_L}} \sigma(\vec{x}, t) \right] d\vec{k} \\
&= \int_{\vec{v}\cdot\eta>0} \vec{v} \cdot \eta f|_+ d\vec{k} + p \int_{\vec{v}\cdot\eta<0} \vec{v} \cdot \eta f'|_+ d\vec{k} + (1-p)\sigma C \int_{\vec{v}\cdot\eta<0} \vec{v} \cdot \eta e^{\frac{-\varepsilon(\vec{k})}{K_B T_L}} d\vec{k} \\
&= \sigma(\vec{x}, t) - p\sigma(\vec{x}, t) + (1-p)\sigma(\vec{x}, t)(-1) = 0.
\end{aligned}$$

However, for $p(\vec{k})$ a function of the crystal momentum the same choice of $\sigma(\vec{x},t)$ and $C(x)$ as in the diffusive case does not necessarily guarantee that the zero flux condition will be satisfied at Neumann boundaries. Therefore, a new condition for C in order to satisfy this condition must be derived. We derive it below.

The general mixed reflection BC can be formulated as

$$f(\vec{x},\vec{k},t)|_- = p(\vec{k})\, f|_+(\vec{x},\vec{k}',t) + (1-p(\vec{k}))\, C'\sigma'\{f|_+\}(\vec{x},t)\, e^{-\varepsilon(\vec{k})/K_BT}, \quad (\vec{x},\vec{k}) \in \Gamma_N^-$$

where $\sigma'\{f|_+\}(\vec{x},t)$ and C' are the function and parameter such that the pointwise zero flux condition is satisfied at the Neumann boundaries

$$\begin{aligned} 0 &= \eta(\vec{x}) \cdot J(\vec{x},t) \\ &= \int_{\vec{v}\cdot\eta>0} \vec{v}\cdot\eta\, f|_+ \, d\vec{k} + \int_{\vec{v}\cdot\eta<0} \vec{v}\cdot\eta \left[p(\vec{k}) f(\vec{x},\vec{k}',t)|_+ + (1-p(\vec{k}))C' e^{\frac{-\varepsilon(\vec{k})}{K_BT_L}} \sigma'(\vec{x},t) \right] d\vec{k}. \end{aligned}$$

Since

$$0 = \int_{\vec{v}\cdot\eta>0} \vec{v}\cdot\eta\, f|_+ \, d\vec{k} + \int_{\vec{v}\cdot\eta<0} \vec{v}\cdot\eta\, p(\vec{k}) f'|_+ \, d\vec{k} - \sigma'(\vec{x},t)\, C' \int_{\vec{v}\cdot\eta<0} (1-p(\vec{k}))|\vec{v}\cdot\eta|\, e^{\frac{-\varepsilon}{K_BT_L}}\, d\vec{k},$$

we conclude then that

$$\sigma'\{f|_+\}(\vec{x},t) = \int_{\vec{v}\cdot\eta>0} \vec{v}\cdot\eta\, f|_+ \, d\vec{k} - \int_{\vec{v}\cdot\eta<0} |\vec{v}\cdot\eta|\, p(\vec{k})\, f(\vec{x},\vec{k}',t)|_+ \, d\vec{k}, \tag{5.54}$$

$$C'\left\{\eta(\vec{x})\right\} = \left(\int_{\vec{v}\cdot\eta<0} (1-p(\vec{k}))|\vec{v}\cdot\eta|\, e^{\frac{-\varepsilon}{K_BT_L}}\, d\vec{k} \right)^{-1}. \tag{5.55}$$

The general mixed reflection BC then has the specific form

$$\begin{aligned} f(\vec{x},\vec{k},t)|_- &= p(\vec{k})\, f|_+(\vec{x},\vec{k}',t) \\ &\quad + (1-p(\vec{k}))e^{-\frac{\varepsilon(\vec{k})}{K_BT}} \frac{\left(\int_{\vec{v}\cdot\eta>0} \vec{v}\cdot\eta f|_+ d\vec{k} - \int_{\vec{v}\cdot\eta<0} |\vec{v}\cdot\eta| p(\vec{k}) f(\vec{x},\vec{k}',t)|_+ d\vec{k} \right)}{\int_{\vec{v}\cdot\eta<0} (1-p(\vec{k}))|\vec{v}\cdot\eta|\, e^{\frac{-\varepsilon(\vec{k})}{K_BT_L}}\, d\vec{k}}, \end{aligned}$$

with $(\vec{x},\vec{k}) \in \Gamma_N^-$, $(\vec{x},\vec{k}') \in \Gamma_N^+$ s.t. $\vec{v}(\vec{k}') = \vec{v}(\vec{k}) - 2(\vec{v}(\vec{k})\cdot\eta)\eta$.

Notice that the product $C'\sigma'(\vec{x},t)$ has the form

$$C'\sigma'(\vec{x},t) = \frac{\left(\int_{\vec{v}\cdot\eta>0} \vec{v}\cdot\eta\, f|_+ \, d\vec{k} - \int_{\vec{v}\cdot\eta<0} |\vec{v}\cdot\eta|\, p(\vec{k})\, f(\vec{x},\vec{k}',t)|_+ \, d\vec{k} \right)}{\int_{\vec{v}\cdot\eta<0} (1-p(\vec{k}))|\vec{v}\cdot\eta|\, e^{\frac{-\varepsilon(\vec{k})}{K_BT_L}}\, d\vec{k}} \tag{5.56}$$

which for the case of p constant, it reduces to the original function $\sigma(\vec{x},t)$ and parameter $C\left\{\eta(\vec{x})\right\}$.

$$\begin{aligned} \text{If} \quad p &= \text{ct}, \\ C'\sigma'(\vec{x},t) &= \frac{\left(\int_{\vec{v}\cdot\eta>0} \vec{v}\cdot\eta\, f|_+ \, d\vec{k} - p \int_{\vec{v}\cdot\eta<0} |\vec{v}\cdot\eta|\, f(\vec{x},\vec{k}',t)|_+ \, d\vec{k} \right)}{\int_{\vec{v}\cdot\eta<0} (1-p)|\vec{v}\cdot\eta|\, e^{\frac{-\varepsilon(\vec{k})}{K_BT_L}}\, d\vec{k}} \\ &= \frac{(1-p) \int_{\vec{v}\cdot\eta>0} \vec{v}\cdot\eta\, f|_+ \, d\vec{k}}{(1-p) \int_{\vec{v}\cdot\eta<0} |\vec{v}\cdot\eta|\, e^{\frac{-\varepsilon(\vec{k})}{K_BT_L}}\, d\vec{k}} \\ &= \frac{\int_{\vec{v}\cdot\eta>0} \vec{v}\cdot\eta\, f|_+ \, d\vec{k}}{\int_{\vec{v}\cdot\eta<0} |\vec{v}\cdot\eta|\, e^{\frac{-\varepsilon(\vec{k})}{K_BT_L}}\, d\vec{k}} \\ &= C\,\sigma\left(\vec{x},t\right). \end{aligned}$$

However, for the non-constant case $p(\vec{k})$ the new function and parameter $\sigma'(\vec{x},t)$, $C'(\eta)$ need to be used instead, as the previous $\sigma(\vec{x},t)$, $C(\eta)$ will not satisfy the zero flux condition in general for $p(\vec{k})$, since

$$0 = \int_{\vec{v}\cdot\eta>0} \vec{v}\cdot\eta f|_+ d\vec{k} + \int_{\vec{v}\cdot\eta<0} \vec{v}\cdot\eta p(\vec{k}) f'|_+ d\vec{k} - \sigma' C' \int_{\vec{v}\cdot\eta<0} (1-p(\vec{k}))|\vec{v}\cdot\eta| e^{\frac{-\varepsilon}{K_B T_L}} d\vec{k}$$

$$C'\sigma' = \frac{\int_{\vec{v}\cdot\eta>0} \vec{v}\cdot\eta\, f|_+ \, d\vec{k} + \int_{\vec{v}\cdot\eta<0} \vec{v}\cdot\eta\, p(\vec{k})\, f(\vec{x},\vec{k}',t)|_+ \, d\vec{k}}{\int_{\vec{v}\cdot\eta<0}(1-p(\vec{k}))|\vec{v}\cdot\eta|\, e^{\frac{-\varepsilon}{K_B T_L}}\, d\vec{k}}$$

$$\neq \frac{\int_{\vec{v}\cdot\eta>0} \vec{v}\cdot\eta\, f|_+ \, d\vec{k}}{\int_{\vec{v}\cdot\eta<0} |\vec{v}\cdot\eta|\, e^{\frac{-\varepsilon(\vec{k})}{K_B T_L}}\, d\vec{k}} = C\sigma(\vec{x},t) \quad \text{in general for } p(\vec{k}).$$

A more general possible case of mixed reflection BC would have a specularity parameter $p(\vec{x},\vec{k},t)$ dependent on position, momentum, and time. The related reflective BC would then be

$$f|_-(\vec{x},\vec{k},t) = p(\vec{x},\vec{k},t) f|_+(\vec{x},\vec{k}',t) + \Big(1-p(\vec{x},\vec{k},t)\Big) C^*(\vec{x},t)\sigma^*(\vec{x},t) M(\vec{x},\vec{k})$$
$$(\vec{x},\vec{k}) \in \Gamma_{N^-}, \text{ and } (\vec{x},\vec{k}') \in \Gamma_{N^+}, \tag{5.57}$$

where $M(\vec{x},\vec{k})$ is the equilibrium probability distribution (not necessarily a Maxwellian) according to which the electrons diffusively reflect on the physical boundary. $\sigma^*(\vec{x},t)$ and $C^*(\vec{x},t)$ are the functions such that the zero flux condition is satisfied pointwise at insulating boundaries

$$0 = \eta(\vec{x}) \cdot \int_{\Omega_{\vec{k}}} \vec{v}(\vec{k}) f d\vec{k} = \int_{\vec{v}\cdot\eta>0} \eta(\vec{x})\cdot\vec{v}(\vec{k}) f|_+ d\vec{k} + \int_{\vec{v}\cdot\eta<0} \eta(\vec{x})\cdot\vec{v}(\vec{k}) f|_- d\vec{k}$$
$$= \int_{\vec{v}\cdot\eta>0} \eta\cdot\vec{v} f|_+ d\vec{k} + \int_{\vec{v}\cdot\eta<0} \eta\cdot\vec{v} \Big[p(\vec{x},\vec{k},t) f'|_+ + (1-p)\, C^*(\vec{x},t)\sigma^*(\vec{x},t) M(\vec{x},\vec{k}) \Big] d\vec{k}$$
$$= \int_{\vec{v}\cdot\eta>0} \eta\cdot\vec{v} f|_+ d\vec{k} + \int_{\vec{v}\cdot\eta<0} \eta\cdot\vec{v}\, p(\vec{x},\vec{k},t) f|_+(\vec{x},\vec{k}',t) d\vec{k}$$
$$- \sigma^*(\vec{x},t)\, C^*(\vec{x},t) \int_{\vec{v}\cdot\eta<0} |\eta\cdot\vec{v}| \Big(1-p(\vec{x},\vec{k},t)\Big) M(\vec{x},\vec{k}) d\vec{k}.$$

Therefore we conclude for this reflection case that

$$\sigma^* \{f|_+\}(\vec{x},t) = \int_{\vec{v}\cdot\eta>0} |\eta\cdot\vec{v}| f|_+ d\vec{k} - \int_{\vec{v}\cdot\eta<0} |\eta\cdot\vec{v}|\, p(\vec{x},\vec{k},t) f|_+(\vec{x},\vec{k}',t) d\vec{k}, \tag{5.58}$$

$$C^*(\vec{x},t) = \left(\int_{\vec{v}\cdot\eta<0} |\eta\cdot\vec{v}| \Big(1-p(\vec{x},\vec{k},t)\Big) M(\vec{x},\vec{k}) d\vec{k} \right)^{-1}, \tag{5.59}$$

and then the full BC formula for the $p(\vec{x},\vec{k},t)$ reflection case is

$$f|_-(\vec{x},\vec{k},t) = p(\vec{x},\vec{k},t) f|_+(\vec{x},\vec{k}',t) \quad +$$
$$\Big(1-p(\vec{x},\vec{k},t)\Big) M(\vec{x},\vec{k}) \frac{\Big[\int_{\vec{v}\cdot\eta>0} |\eta\cdot\vec{v}| f|_+ d\vec{k} - \int_{\vec{v}\cdot\eta<0} |\eta\cdot\vec{v}|\, p(\vec{x},\vec{k},t) f|_+(\vec{x},\vec{k}',t) d\vec{k}\Big]}{\int_{\vec{v}\cdot\eta<0} |\eta\cdot\vec{v}| \Big(1-p(\vec{x},\vec{k},t)\Big) M(\vec{x},\vec{k}) d\vec{k}}.$$

Remark: $p(\vec{x},\vec{k},t)$ can be any iid random variable in $(\vec{x},\vec{k},t)$.

5.3.1. Numerical implementation

The numerical implementation of the general mixed reflection with specularity parameter $p(\vec{k})$ is done in such a way that a numerical equivalent of the pointwise zero flux condition is achieved.

The general mixed reflection boundary condition in our DG numerical scheme is

$$\Phi_h|_- = \Pi_h \left\{ F_M \left(\Phi_h|_+ \right) \right\} \tag{5.60}$$
$$= \Pi_h \left\{ p(\vec{w}) \Phi_h|_+(\vec{x},\vec{w}',t) + (1-p(\vec{w})) C' \sigma'_h \{\Phi_h|_+\}(\vec{x},t)\, e^{-w} s(w) \right\}.$$

We will be using the notation

$$\vec{w} = (w, \mu, \varphi), \quad d\vec{w} = dw\, d\mu\, d\varphi\,, \quad \vec{w}' = (w, \mu, \pi - \varphi). \tag{5.61}$$

The specific form of C' and σ' will be deduced from the numerical analogous of the mixed reflection boundary condition. We want to satisfy numerically the zero flux condition

$$\begin{aligned} 0 &= \eta(\vec{x}) \cdot \int_{\Omega_{\vec{w}}} \vec{v}(\vec{w})\, \Phi_h d\vec{w} \qquad (5.62)\\ &= \int_{\vec{v}\cdot\eta>0} \vec{v}(\vec{w}) \cdot \eta\, \Phi_h|_+ d\vec{w} + \int_{\vec{v}\cdot\eta<0} \vec{v}(\vec{w}) \cdot \eta\, \Phi_h|_- d\vec{w}\\ &= \int_{\vec{v}\cdot\eta>0} \vec{v}\cdot\eta\, \Phi_h|_+ d\vec{w} + \int_{\vec{v}\cdot\eta<0} \vec{v}\cdot\eta\, \Pi_h \left\{ p(\vec{w})\Phi_h'|_+ + (1-p(\vec{w}))C'\sigma_h'(\vec{x},t)e^{-w}s(w) \right\} d\vec{w}\\ &= \int_{\vec{v}\cdot\eta>0} \vec{v}\cdot\eta\, \Phi_h|_+ d\vec{w} - \int_{\vec{v}\cdot\eta<0} |\vec{v}\cdot\eta|\, \Pi_h \left\{ p(\vec{w})\Phi_h|_+(\vec{x},\vec{w}',t) \right\} d\vec{w}\\ &+ \int_{\vec{v}\cdot\eta<0} \vec{v}\cdot\eta\, \Pi_h \left\{ (1-p(\vec{w}))C'\sigma_h'(\vec{x},t)e^{-w}s(w) \right\} d\vec{w}. \qquad (5.63) \end{aligned}$$

In the space V_h of piecewise continuous polynomials which are tensor products of polynomials of degree p in $\vec{x}$ and of degree q in $\vec{w}$, it holds that

$$\begin{aligned} &\Pi_h \left\{ f_1(\vec{x}) f_2(\vec{w}) \right\} = \Pi_h \left\{ f_1(\vec{x}) \right\} \Pi_h \left\{ f_2(\vec{w}) \right\}, \qquad (5.64)\\ &V_h = \{ v : v|_{\Omega_{ijkmn}} \in Q^{p,q}(\Omega_{ijkmn}) = P^p(X_{ij}) \otimes P^q(K_{kmn}) \}. \end{aligned}$$

Therefore, we have for our particular case that

$$\Pi_h \left\{ (1-p(\vec{w}))C'\sigma_h'(\vec{x},t)e^{-w}s(w) \right\} = C'\sigma_h'(\vec{x},t) \left[\sum_{k,m,n} \chi_{kmn} \frac{\int_{K_{kmn}} (1-p(\vec{w}))e^{-w}s(w)d\vec{w}}{\int_{K_{kmn}} d\vec{w}} \right]$$

Using this, our numerical pointwise zero flux condition is

$$\begin{aligned} 0 &= \int_{\vec{v}\cdot\eta>0} \vec{v}\cdot\eta\, \Phi_h|_+ d\vec{w} - \int_{\vec{v}\cdot\eta<0} |\vec{v}\cdot\eta|\, \Pi_h \left\{ p(\vec{w})\Phi_h|_+(\vec{x},\vec{w}',t) \right\} d\vec{w}\\ &+ \int_{\vec{v}\cdot\eta<0} \vec{v}\cdot\eta\, C'\sigma_h'(\vec{x},t) \left[\sum_{k,m,n} \chi_{kmn} \frac{\int_{K_{kmn}} (1-p(\vec{w}))e^{-w}s(w)d\vec{w}}{\int_{K_{kmn}} d\vec{w}} \right] d\vec{w}\\ &= \int_{\vec{v}\cdot\eta>0} \vec{v}\cdot\eta\, \Phi_h|_+ d\vec{w} - \int_{\vec{v}\cdot\eta<0} |\vec{v}\cdot\eta|\, \Pi_h \left\{ p(\vec{w})\Phi_h|_+(\vec{x},\vec{w}',t) \right\} d\vec{w}\\ &+ C'\sigma_h'(\vec{x},t) \int_{\vec{v}\cdot\eta<0} \vec{v}\cdot\eta \left[\sum_{k,m,n} \chi_{kmn} \frac{\int_{K_{kmn}} (1-p(\vec{w}))e^{-w}s(w)d\vec{w}}{\int_{K_{kmn}} d\vec{w}} \right] d\vec{w}\\ &= \int_{\vec{v}\cdot\eta>0} \vec{v}\cdot\eta\, \Phi_h|_+ d\vec{w} - \int_{\vec{v}\cdot\eta<0} |\vec{v}\cdot\eta|\, \Pi_h \left\{ p(\vec{w})\Phi_h|_+(\vec{x},\vec{w}',t) \right\} d\vec{w}\\ &- C'\sigma_h'(\vec{x},t) \sum_{k,m,n} \chi_{kmn} \int_{\vec{v}\cdot\eta<0} |\vec{v}\cdot\eta|\, d\vec{w}\, \frac{\int_{K_{kmn}} (1-p(\vec{w}))e^{-w}s(w)d\vec{w}}{\int_{K_{kmn}} d\vec{w}}\\ &= \int_{\vec{v}\cdot\eta>0} \vec{v}\cdot\eta\, \Phi_h|_+ d\vec{w} - \int_{\vec{v}\cdot\eta<0} |\vec{v}\cdot\eta|\, \Pi_h \left\{ p(\vec{w})\Phi_h|_+(\vec{x},\vec{w}',t) \right\} d\vec{w} \end{aligned}$$

$$- \sigma_h'(\vec{x},t)\, C' \sum_{k,m,n,\ \vec{v}\cdot\eta<0} \int_{K_{kmn}} |\vec{v}\cdot\eta|\, d\vec{w}\, \frac{\int_{K_{kmn}} (1-p(\vec{w}))e^{-w} s(w) d\vec{w}}{\int_{K_{kmn}} d\vec{w}}\,.$$

We conclude then that we can achieve a numerical equivalent of the pointwise zero flux condition by defining

$$\sigma_h' \{\Phi_h|_+\}(\vec{x},t) = \int_{\vec{v}\cdot\eta>0} \vec{v}\cdot\eta\, \Phi_h|_+ d\vec{w} - \int_{\vec{v}\cdot\eta<0} |\vec{v}\cdot\eta|\, \Pi_h\left\{p(\vec{w})\Phi_h|_+(\vec{x},\vec{w}',t)\right\} d\vec{w},$$

$$\left(C'\{\eta\}\right)^{-1} = \sum_{k,m,n,\ \vec{v}\cdot\eta<0} \int_{K_{kmn}} |\vec{v}\cdot\eta|\, d\vec{w}\, \frac{\int_{K_{kmn}} (1-p(\vec{w}))e^{-w} s(w) d\vec{w}}{\Delta w_k \Delta\mu_m \Delta\varphi_n}\,. \tag{5.65}$$

Therefore, the inflow BC in our DG numerical method is given by the expression

$$\begin{aligned}\Phi_h|_- &= \Pi_h\left\{p(\vec{w})\Phi_h|_+(\vec{x},\vec{w}',t)\right\} \\ &+ \Pi_h\left\{(1-p(\vec{w}))C'\left(\int_{\vec{v}\cdot\eta>0} \vec{v}\cdot\eta\,\Phi_h|_+ d\vec{w}\right.\right. \\ &\left.\left. - \int_{\vec{v}\cdot\eta<0} |\vec{v}\cdot\eta|\,\Pi_h\left\{p(\vec{w})\Phi_h|_+(\vec{x},\vec{w}',t)\right\} d\vec{w}\right) e^{-w} s(w)\right\}.\end{aligned}$$

The particular form of the coefficients defining the piecewise polynomial approximation $\Phi_h|_-$ for the general mixed reflection BC is presented below for the boundary $y = L_y$, since the calculations for the case of the boundary $y = 0$ are analogous.

For the boundary $y_{N_y+1/2} = L_y\,, \quad \eta\cdot\vec{v} \propto +\hat{y}\cdot\vec{g} = g_2 \propto \cos\varphi$, which defines the sign of g_2. Outflow cells have the index $j = N_y$. They are cells inside the domain adjacent to the boundary. Inflow cells have the index $j = N_y + 1$. They are ghost cells adjacent to the boundary. We have in our case that

$$\begin{aligned}\sigma_h' &= \int_{\cos\varphi>0} g_2\,\Phi_h|_+ d\vec{w} - \int_{\cos\varphi<0} |g_2|\,\Pi_h\left\{p(\vec{w})\Phi_h|_+(\vec{x},\vec{w}',t)\right\} d\vec{w} \\ &= \sum_{k,m,n}^{n\le\frac{N_\varphi}{2}} \int_{K_{kmn}} g_2\,\Phi_h|_+ d\vec{w} - \sum_{k,m,n}^{n>\frac{N_\varphi}{2}} \int_{K_{kmn}} |g_2|\,\Pi_h\left\{p(\vec{w})\Phi_h|_+(\vec{x},\vec{w}',t)\right\} d\vec{w}\,.\end{aligned}$$

If $I = (i, N_y+1, k, m, n)$ (inflow), $I' = (i, N_y, k, m, n')$, $n' = N_\varphi' - n + 1$ (outflow), the projection integrand is given by

$$\Pi_h\left\{p(\vec{w})\Phi_h|_+(\vec{x},\vec{w}',t)\right\} = \sum_I^{n>N_\varphi/2} \chi_I \frac{\int_{kmn} p(\vec{w}) d\vec{w}}{\int_{kmn} d\vec{w}} \left[T_{I'} + X_{I'}\frac{(x-x_i)}{\Delta x_i/2} + Y_{I'}(+1)\right].$$

The coefficients of σ_h' are given below. We have now that $I = (i, N_y, k, m, n)$, $I' = (i, N_y, k, m, n')$, $\quad n' = N_\varphi' - n + 1$, so from the previous two formulas then

$$\begin{aligned}\sigma'^{0}_{i,N_y} &= \sum_{k,m,n}^{n\le N_p/2} T_I(t) \int_k \frac{\sqrt{w(1+\alpha_K w)}}{1+2\alpha_K w} dw \int_m \sqrt{1-\mu^2} d\mu \int_n \cos\varphi d\varphi \\ &- \sum_{k,m,n}^{n>N_p/2} T_{I'}(t) \int_k \frac{\sqrt{w(1+\alpha_K w)}}{1+2\alpha_K w} dw \int_m \sqrt{1-\mu^2} d\mu \int_n |\cos\varphi| d\varphi\, \frac{\int_{kmn} p(\vec{w}) d\vec{w}}{\int_{kmn} d\vec{w}}, \\ \sigma'^{x}_{i,N_y} &= \sum_{k,m,n}^{n\le N_p/2} X_I(t) \int_k \frac{\sqrt{w(1+\alpha_K w)}}{1+2\alpha_K w} dw \int_m \sqrt{1-\mu^2} d\mu \int_n \cos\varphi d\varphi \\ &- \sum_{k,m,n}^{n>N_p/2} X_{I'}(t) \int_k \frac{\sqrt{w(1+\alpha_K w)}}{1+2\alpha_K w} dw \int_m \sqrt{1-\mu^2} d\mu \int_n |\cos\varphi| d\varphi\, \frac{\int_{kmn} p(\vec{w}) d\vec{w}}{\int_{kmn} d\vec{w}},\end{aligned} \tag{5.66}$$

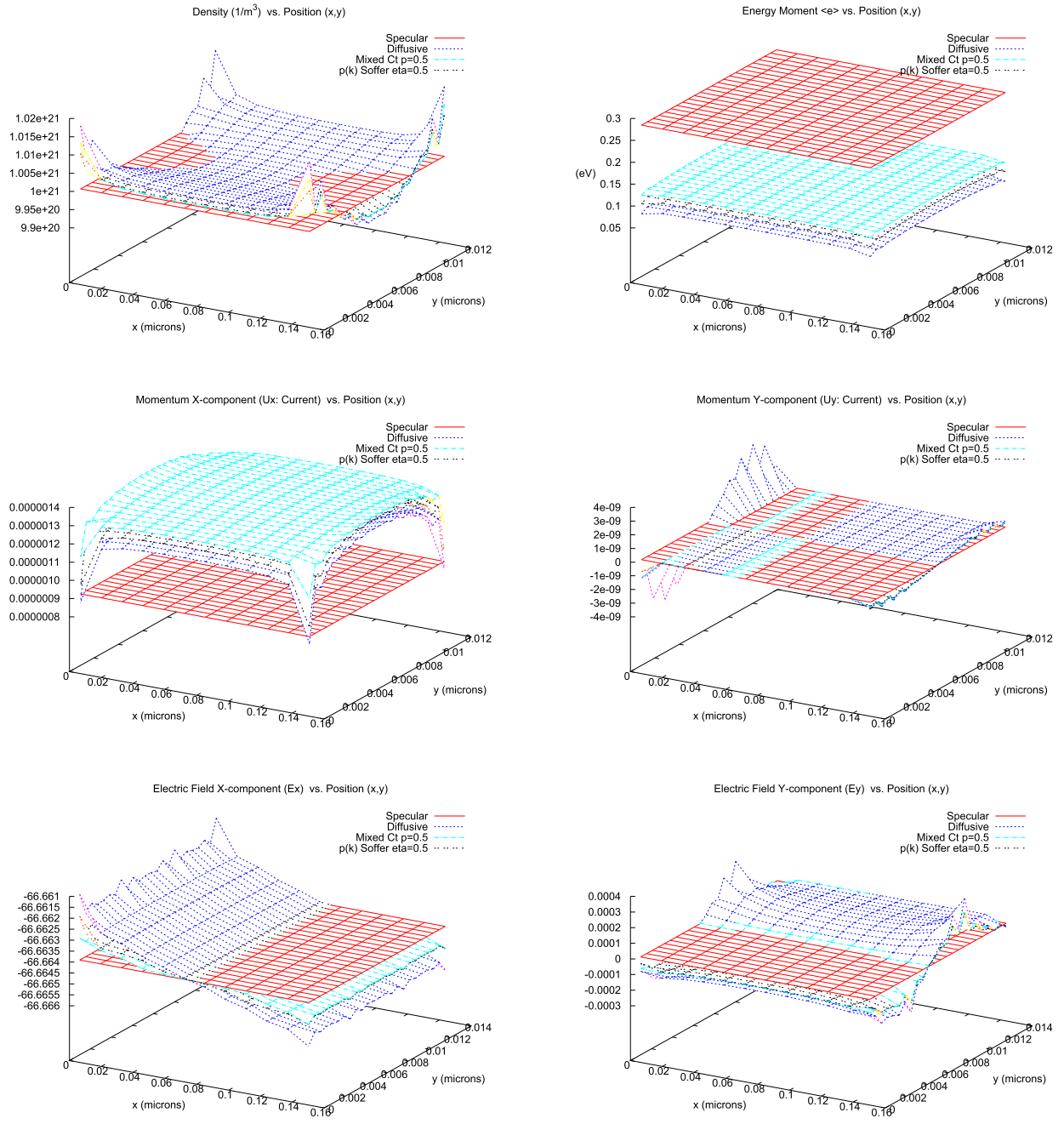

Fig. 6.2. Density ρ (m^{-3}), Mean energy e (eV), Momentum U_x, U_y (10^{28} $\frac{\mathrm{cm}^{-2}}{\mathrm{s}}$), Electric Field Components E_x and E_y, and Potential V (Volts) vs Position (x, y) in (μm) plot for Specular, Diffusive, Mixed $p = 0.5$ & Mixed $p(\vec{k}) = \exp(-4\eta^2|k|^2\sin^2\varphi)$, $\eta = 0.5$ Reflection for 2D bulk silicon.

$$\sigma'^{y}_{i,N_y} = \sum_{k,m,n}^{n\le N_p/2} Y_I(t) \int_k \frac{\sqrt{w(1+\alpha_K w)}}{1+2\alpha_K w} dw \int_m \sqrt{1-\mu^2}\, d\mu \int_n \cos\varphi\, d\varphi$$
$$- \sum_{k,m,n}^{n>N_p/2} Y_{I'}(t) \int_k \frac{\sqrt{w(1+\alpha_K w)}}{1+2\alpha_K w} dw \int_m \sqrt{1-\mu^2}\, d\mu \int_n |\cos\varphi| d\varphi \, \frac{\int_{kmn} p(\vec{w}) d\vec{w}}{\int_{kmn} d\vec{w}}.$$

Since on one hand we have

$$\Phi_h|^-_{L_y} = \Pi_h\left\{p(\vec{w})\Phi_h|_+(\vec{x},\vec{w}',t)\right\} + \Pi_h\left\{(1-p(\vec{w}))C'\sigma'_h\{\Phi_h|_+\}(\vec{x},t)\, e^{-w} s(w)\right\}$$

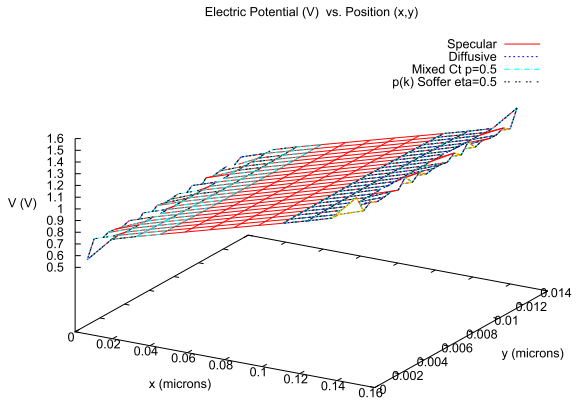

Fig. 6.2. (*continued*)

$$
\begin{aligned}
&= \sum_{ikmn}^{n>\frac{N_\varphi}{2}} \chi_{i,N_y+1,kmn} \frac{\int_{kmn} p\, d\vec{w}}{\int_{kmn} d\vec{w}} \left[T_{i,N_y,k,m,n'} + X_{i,N_y,k,m,n'} \frac{(x-x_i)}{\Delta x_i/2} + Y_{i,N_y,k,m,n'} \right] \\
&+ \sum_{i,k,m,n}^{n>N_\varphi/2} \chi_{i,N_y+1,k,m,n} \frac{\int_{kmn} (1-p(\vec{w}))e^{-w} s(w) d\vec{w}}{\int_{kmn} d\vec{w}} \times \\
&\times C' \left[\sigma'^{0}_{i,N_y} + \sigma'^{x}_{i,N_y} \frac{(x-x_i)}{\Delta x_i/2} + \sigma'^{y}_{i,N_y}(+1) \right],
\end{aligned}
$$

and on the other hand

$$
\Phi_h|^{-}_{y_{N_y+1/2}} = \sum_{i,k,m,n}^{n>\frac{N_\varphi}{2}} \chi_{i,N_y+1,k,m,n} \left[T_{i,N_y+1,k,m,n} + X_{i,N_y+1,k,m,n} \frac{(x-x_i)}{\Delta x_i/2} - Y_{i,N_y+1,k,m,n} \right],
$$

we conclude that the coefficients for $\Phi_h|_-$ are

$$
\begin{aligned}
T_{i,N_y+1,k,m,n} &= T_{I'} \frac{\int_{kmn} p(\vec{w}) d\vec{w}}{\int_{kmn} d\vec{w}} + C' \sigma'^{0}_{i,N_y} \frac{\int_{kmn} (1-p(\vec{w}))e^{-w} s(w) d\vec{w}}{\int_{kmn} d\vec{w}}, \\
X_{i,N_y+1,k,m,n} &= X_{I'} \frac{\int_{kmn} p(\vec{w}) d\vec{w}}{\int_{kmn} d\vec{w}} + C' \sigma'^{x}_{i,N_y} \frac{\int_{kmn} (1-p(\vec{w}))e^{-w} s(w) d\vec{w}}{\int_{kmn} d\vec{w}}, \\
Y_{i,N_y+1,k,m,n} &= -\left(Y_{I'} \frac{\int_{kmn} p(\vec{w}) d\vec{w}}{\int_{kmn} d\vec{w}} + C' \sigma'^{y}_{i,N_y} \frac{\int_{kmn} (1-p(\vec{w}))e^{-w} s(w) d\vec{w}}{\int_{kmn} d\vec{w}} \right), \\
I' &= (i, N_y, k, m, n'), \quad I = (i, N_y, k, m, n).
\end{aligned} \tag{5.67}
$$

6. Numerical results

6.1. 2D bulk silicon

We present results of numerical simulations for the case of n 2D bulk silicon diode with an applied bias between the boundaries $x = 0$, L_x, and reflection BC at the boundaries $y = 0$, L_y (Figs. 6.2). The required dimensionality in momentum space is a 3D $\vec{k}(w, \mu, \varphi)$. The specifics of our simulations are:
Initial Condition: $\Phi(w)|_{t=0} = \Pi_h \left\{ Ne^{-w} s(w) \right\}$. Final Time: 1.0 ps.
Boundary Conditions (BC):
$\vec{k}$-space: Cut-off – at $w = w_{max}$, Φ is machine zero.
Only needed BC in (w, μ, φ): transport normal to the boundary analytically zero at 'singular points' boundaries:
At $w = 0$, $g_3 = 0$. At $\mu = \pm 1$, $g_4 = 0$. At $\varphi = 0, \pi$, $g_5 = 0$.
$\vec{x}$-space: Charge Neutrality at boundaries $x = 0$, $x = 0.15$ μm.
Bias-Potential: $V|_{x=0} = 0.5235$ V, $V|_{x=0.15\ \mu m} = 1.5235$ V.
Neumann BC for Potential at $y = 0$, $L_y = 12$ nm: $\partial_y V|_{y=0,\, L_y} = 0$.

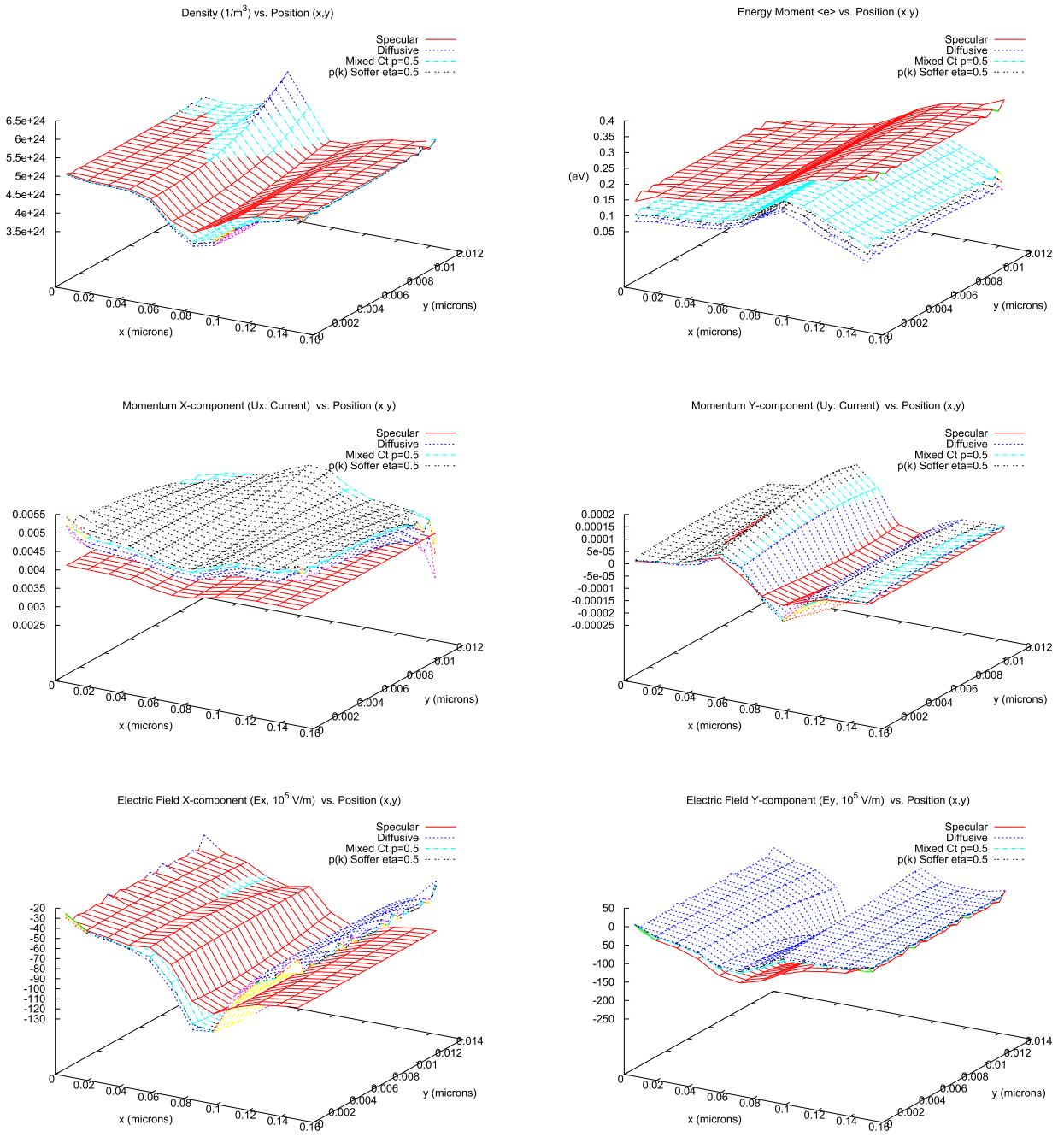

Fig. 6.3. Density ρ (m^{-3}), Mean energy e (eV), Momentum U_x, U_y (10^{28} $\frac{\mathrm{cm}^{-2}}{\mathrm{s}}$), Electric Field Components E_x and E_y, and Potential V (Volts) vs Position (x, y) in (μm) plot for Specular, Diffusive, Mixed $p = 0.5$ & Mixed $p(\vec{k}) = \exp(-4\eta^2|k|^2 \sin^2\varphi)$, $\eta = 0.5$ Reflection for a 2D double gated MOSFET.

Reflection BC at $y = 0, y = 12$ nm: Specular, Diffusive, Mixed Reflection with constant specularity $p = 0.5$, and Mixed Reflection using a momentum dependent specularity $p(\vec{k}) = \exp(-4\eta^2|k|^2 \sin^2\varphi)$, the nondimensional roughness rms height coefficient being $\eta = 0.5$.

We observe an influence of the Diffusive and Mixed Reflection in macroscopic observables. It is particularly noticeable in the kinetic moments. For example, the charge density slightly increases with diffusivity close to the reflecting boundaries, and, due to mass conservation, alters the density profile over the domain. Momentum & mean velocity increase with diffusive reflection over the domain, while the energy is decreased by diffusive reflection over the domain. There is a negligible difference in the electric field x component below its orders of magnitude for the different reflection cases.

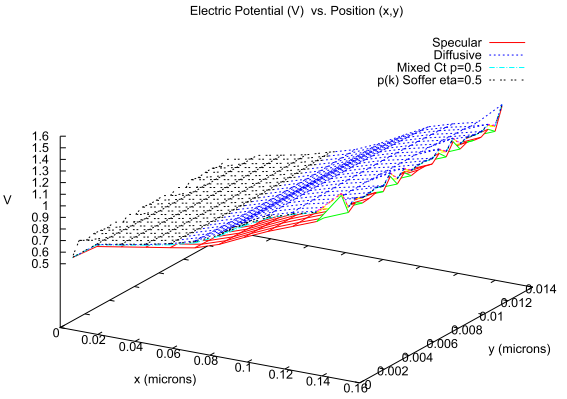

Fig. 6.3. (*continued*)

6.2. 2D double gated MOSFET

We present as well the results of numerical simulations for the case of a 2D double gated MOSFET device (Figs. 6.3). On one hand, the BC for the Poisson Eq. for this device would be the Dirichlet BC $\Psi = 0.5235$ Volts at the source $x = 0$, $\Psi = 1.5235$ Volts at the drain $x = L_x$, and $\Psi = 1.06$ Volts at the gates. On the other hand, Homogeneous Neumann BC $\partial_{\hat{n}}\Psi = 0$ are imposed at the rest of the boundaries. Specular reflection is applied at the boundary $y = 0$ because the solution is symmetric with respect to $y = 0$ for our 2D double gate MOSFET (Fig. 4.1). At the boundary $y = L_y$ we apply specular, diffusive, and mixed reflection BC, both with constant $p = 0.5$, and with a momentum dependent $p(\vec{k}) = \exp(-4\eta^2|k|^2\sin^2\varphi)$ with roughness coefficient $\eta = 0.5$. We use again the initial condition: $\Phi(w)|_{t=0} = \Pi_h\left\{N_D(x,y)e^{-w}s(w)\right\}$, running the simulations up to the physical time of 1.0 ps. We use again as well a cut-off BC in the boundary of the momentum domain, so Φ is machine zero at $w = w_{max}$, and we apply charge neutrality BC at $x = 0$, $x = 0.15$ μm.

We observe a quantitative difference in the kinetic moments and other observables between the different cases of reflective BC, with the physical quantities being of the same order of magnitude. The electron density increases close to the gates with diffusive reflection, and close to the center of the device, given by the boundary $y = 0$, the density profile is greater for specular reflection. The energy moment clearly decreases with diffusive reflection over the physical domain. The momentum x-component for specular reflection is less than for the other reflective cases. There is a difference in the profile of the electric field x-component between the specular reflection and the other cases that include diffusivity, increasing it with diffusive reflection close to the drain. The electric field y-component increases with diffusive reflection close to the boundary $y = 0$ representing the center of the device. The electric potential is greater for the cases including diffusive reflection than for the perfectly specular case.

6.3. Electrons reentering the 2D domain with reflective BC in y and periodic BC in x: comparison of bulk silicon with collisionless plasma

We consider in this case almost the same physical situation and parameters for the previous section on the 2D bulk silicon, except that instead of using the charge neutrality conditions we apply periodic boundary conditions in the x-boundaries, simulating then that the electrons reenter the material on the opposite x-boundary after the outflow exits the domain. We compare these simulations with ones in which no collisions are considered, corresponding the latter to the case of a collisionless plasma with reflective BC in y and periodic BC in x. For both cases, bulk silicon with electron–phonon collisions and the collisionless electron gas, we still apply an external potential such that $V = 0$ at $x = 0$ and $V = 1$ Volt at $x = L_x$. This can be understood in the framework of periodic BC in x as a periodic sawtooth wave with period equal to the length of the x-domain. We do this comparison in order to study the effect of the reflective boundary conditions in y, with and without the influence of the collisions over electrons, and we let the electrons re-enter the domain under periodic boundary conditions in x, eliminating then the charge neutrality conditions in x and any possible effect due to the latter. Since due to the periodic BC in x the electrons re-enter the domain after they exit it in outflow, the effect of boundary conditions is exclusively related to the reflection in the transport domain in the y-boundaries. For example, in Figs. 6.6 we present the plots of Relative Mass vs Time (ps) for Specular, Diffusive, Mixed with constant and momentum dependent specularity for different sets of simulations. The top figure is related to simulations for bulk silicon with charge neutrality conditions on the non-reflecting boundaries, the middle figure is associated to simulations for bulk silicon with periodic boundary conditions on the non-reflecting boundaries, and the bottom figure is related to the simulations for collisionless electron transport with periodic boundary conditions on the non-reflecting boundaries. The last two sets of simulations mentioned conserve the mass during all the time, and these sets isolate the effect of reflection boundary conditions by using periodic boundary

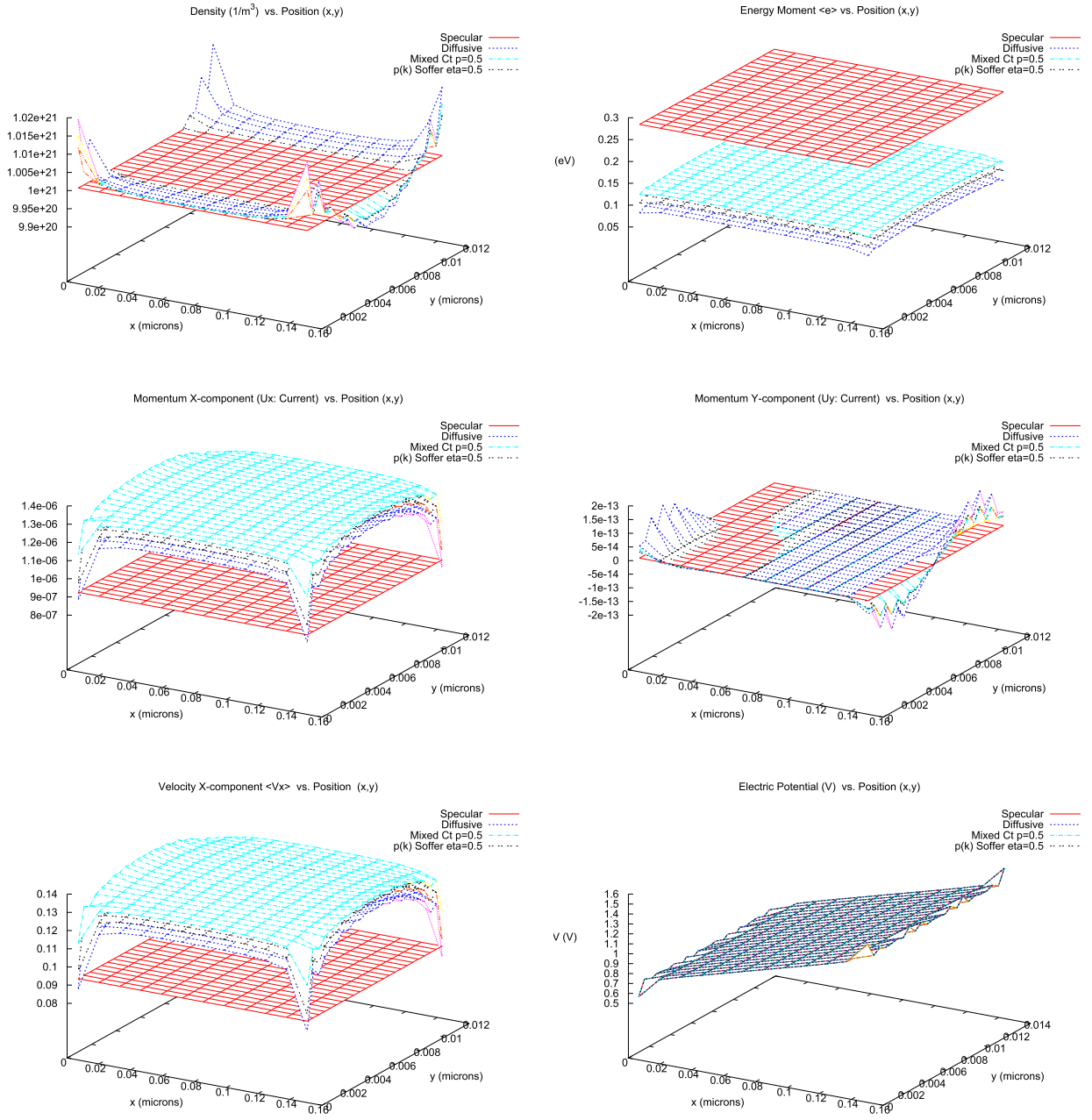

Fig. 6.4. Density ρ (m^{-3}), Mean energy e (eV), Momentum U_x, U_y (10^{28} $\frac{\mathrm{cm}^{-2}}{\mathrm{s}}$), Average Velocity Component V_x, and Potential V (Volts) vs Position (x, y) in (μm) plot for Specular, Diffusive, Mixed $p = 0.5$ & Mixed $p(\vec{k}) = \exp(-4\eta^2|k|^2 \sin^2\varphi)$, $\eta = 0.5$ Reflection for electrons in 2D bulk silicon with reflective BC in y and periodic BC in x.

conditions instead of charge neutrality conditions. The first set associated to charge neutrality conditions in addition to reflection boundary conditions, however, have a slight increase in the relative mass of less than 0.5%. This slight increase then is associated only to the inclusion of charge neutrality conditions and a possible accumulation of numerical error due solely to it.

We notice in our comparison then the following effects of the collision operator in comparison with the collisionless plasma case. As expected, the main effect of collisions is to decrease the magnitude of the average energy, average velocity and momentum (therefore the current) of electrons over the domain (Fig. 6.4). The effect of collisions on the distribution of the electron density profile over the domain is negligible. Regarding the isolated effects of the reflection boundary conditions in the kinetic moments and other physical observables of interest by considering the collisionless plasma with periodic BC in x, we notice, as earlier in the section for bulk silicon, the slight

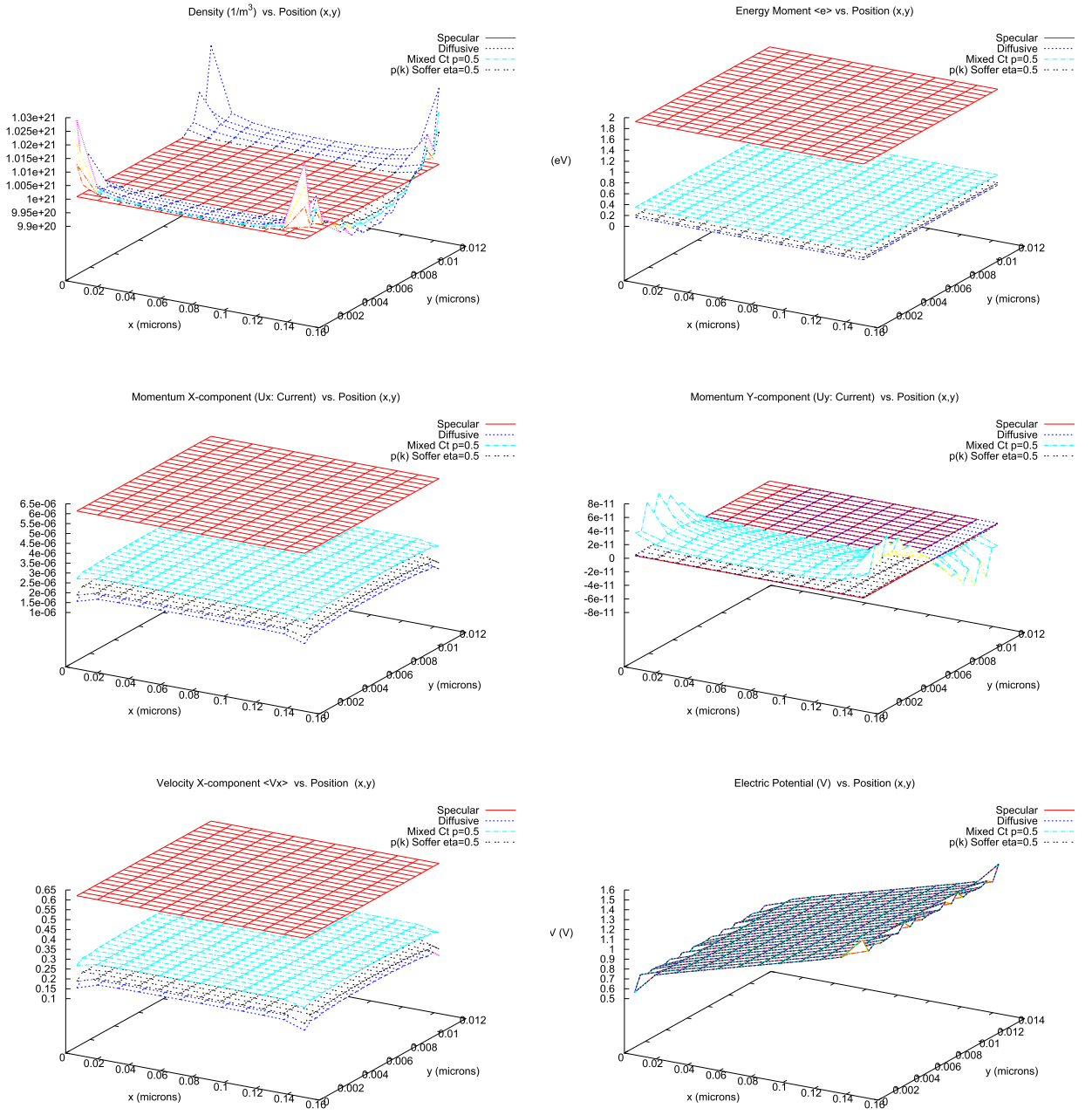

Fig. 6.5. Density ρ (m^{-3}), Mean energy e (eV), Momentum U_x, U_y (10^{28} $\frac{\mathrm{cm}^{-2}}{\mathrm{s}}$), Average Velocity Component V_x, and Potential V (Volts) vs Position (x, y) in (μm) plot for Specular, Diffusive, Mixed $p = 0.5$ & Mixed $p(\vec{k}) = \exp(-4\eta^2|k|^2 \sin^2\varphi)$, $\eta = 0.5$ Reflection for 2D collisionless electrons with reflective BC in y and periodic BC in x.

increase of the density profile close to the reflecting boundaries when adding diffusivity in the boundary conditions, and by conservation of mass, a decrease of the density profile over the center of the domain. The mean energy decreases over the position domain with the inclusion of diffusive reflection BC, as well as the x components (which are the dominant) of the momentum and velocity (Fig. 6.5). It is important to notice this expected effect of the isolated reflection BC in the collisionless plasma case, since for the case that includes electron–phonon collisions combined with adding diffusive reflection BC gives actually an increase in the x components of the momentum and velocity compared to the purely specular reflection case (Fig. 6.4). The collisionless plasma with periodic BC in x and reflection BC in y isolates the effect of the latter then and shows the expected behavior of a decrease in the mean energy, velocity and momentum x-components when adding diffusivity in the reflection boundary conditions.

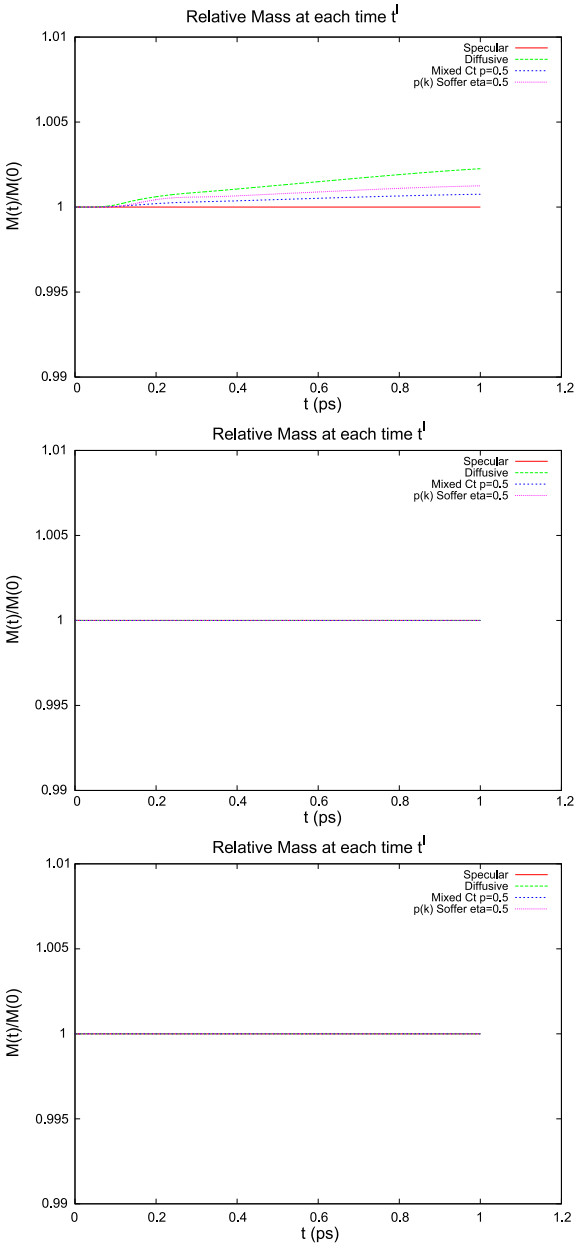

Fig. 6.6. Relative Mass vs Time (ps) plot for Specular, Diffusive, Mixed $p = 0.5$ & Mixed $p(\vec{k}) = \exp(-4\eta^2|k|^2 \sin^2\varphi)$, $\eta = 0.5$ Reflection. The figure on top is related to the simulations for bulk silicon with charge neutrality conditions on the non-reflecting boundaries. The figure in the middle is associated to the simulations for bulk silicon with periodic boundary conditions on the non-reflecting boundaries. The bottom figure is related to the simulations for collisionless electron transport with periodic boundary conditions on the non-reflecting boundaries. The figures show the conservation of mass when isolating the effect of reflection boundary conditions in the simulations, as the slight increase in the relative mass of less than 0.5% is associated only to simulations that also include charge neutrality conditions and possibly an accumulation of numerical error due solely to it.

7. Conclusions

We have considered the mathematical and numerical modeling of Reflective Boundary Conditions in 2D devices and their implementation in DG-BP schemes. We have studied the specular, diffusive and mixed reflection BC on the boundaries of the position domain of the device. We developed a numerical equivalent of the zero flux condition at the position domain boundaries for the case of a more general mixed reflection with a momentum dependant specularity parameter $p(\vec{k})$. We compared the influence of these different reflection cases in the computational prediction of moments after implementing numerical BC equivalent to the respective reflective BC, each one satisfying a mathematical zero flux condition at insulating boundaries. There are effects due to the inclusion of diffusive reflection boundary conditions over the moments and physical

observables of the probability density function, whose influence is not only restricted to the boundaries but actually to the whole domain. Particularly noticeable effects of the inclusion of diffusivity in kinetic moments are the increase of the density close to the reflecting boundary, the decrease of the mean energy over the domain and, in the case when electron–phonon collisions for silicon are included, the increase of the x-components of the mean velocity and momentum over the domain, whereas for the collisionless case, for which only the effects of the reflection boundary conditions are considered (such as when electrons are allowed to reenter the material via periodic boundary conditions in x), a decrease in those x-components of mean velocity and momentum is observed, as expected when adding diffusivity to the reflection boundary conditions.

To summarize, specular boundary conditions have the physical meaning of a reflection with a perfectly smooth surface with no roughness. Diffusive boundary conditions are the opposite case, with the physical meaning of a rough surface that completely diffuses the momentum. That means, for a fixed $\vec{x}$ at a time t, since $f|_-(\vec{x},\vec{k},t) = C\sigma(\vec{x},t)\exp(-\varepsilon(\vec{k}))$, the probability density function is higher for momentum vectors with a lower energy band value, therefore the momentum with the highest $f|_-(\vec{x},\vec{k},t)$ value, for that given $\vec{x}$ at time t, occurs at $\vec{k}=\vec{0}$, where the origin of the momentum space has been chosen as the position of the local energy band valley. Hence, our physical interpretation of the diffusive reflection condition is that it diffuses the momentum giving a higher probability for lower magnitude momentum values, with highest probability density value at $\vec{k}=\vec{0}$. The mixed reflection condition is a convex combination of both, meaning that the reflection process is partially specular and partially diffuses the momentum, with the probability of specularity potentially depending on the momentum variable. Estimating which boundary condition is more physical, we believe mixed reflection case may be the most suitable, as no surface is in practice perfectly specular, and the diffusive reflection is the case in the other end of the spectrum that minimizes the total reflected momentum. Regarding on how to understand the quantitative differences between the output for the considered boundary conditions, we propose, in Section 6.3, a numerical study of the different reflection conditions for collisionless electrons with periodic conditions on the other two boundaries. This case provides the best understanding of the boundary condition role in the simulation as it isolates effects of the reflection conditions, since there is no dissipation from collision mechanisms, and the electrons reenter the domain after exiting a periodic boundary. In fact, we show in Figs. 6.5 that the diffusivity in the boundary condition, as expected, lowers the momentum in the main direction of transport of the electrons, which is $\hat{x}$ (the transport in the $\hat{y}$ direction is negligible), and it also lowers the energy average. Both of these quantitative differences are expected from the reflection of the electrons with a rough boundary. Regarding the quantitative difference between the density output, we observe that particles tend to stay closer to the rough boundaries when increasing the degree of diffusivity in the boundary condition, since the diffusivity decreases the total reflected momentum as it is more probable to have a reflected momentum with lower magnitudes. Therefore the density profile increases for more diffusive conditions as it tends to accumulate more particles in the boundary by lowering their momentum after reflection.

Future research will consider, for example, the inclusion of surface roughness scattering mechanisms in the collision operator for our diffusive reflection problem in silicon devices. It will be related as well to the inclusion of diffusive reflection BC with a DG-BP-EPM full energy band. More importantly, another line of work of our interest for future research will be the more general case of a $p(\vec{x},\vec{k})$ specular probability dependant on momentum and position as well, considering in addition to its mathematical aspects the related numerical issues and the respective computational modeling, intending to use experimental values of $p(\vec{x},\vec{k})$ as input for the simulations.

Acknowledgements

The authors' research was partially supported by NSF grants NSF CHE-0934450, NSF-RNMS DMS-1107465 and DMS 143064, and the ICES Moncrief Grand Challenge Award. The computational work was partially performed by means of TACC resources under project A-ti4. Support from the Institute of Computational Engineering and Sciences and the University of Texas at Austin is gratefully acknowledged.

References

[1] Y. Sone, Molecular Gas Dynamics: Theory, Techniques, and Applications, Birkhauser, 2007.
[2] A. Jüngel, Transport Equations for Semiconductors, Springer Verlag, 2009.
[3] C. Cercignani, The Boltzmann equation and its applications, Appl. Math. Sci. 67 (1988).
[4] C. Cercignani, I.M. Gamba, C.D. Levermore, High field approximations to a Boltzmann–Poisson system and boundary conditions in a semiconductor, Appl. Math. Lett. 10 (4) (1997) 111–117.
[5] S. Soffer, Statistical model for the size effect in electrical conduction, J. Appl. Phys. 38 (1967) 1710.
[6] K. Fuchs, Proc. Camb. Philol. Soc. 34 (1938) 100.
[7] R.F. Greene, Boundary conditions for electron distributions at crystal surfaces, Phys. Rev. 141 (1966) 687.
[8] R.F. Greene, R.W. O'Donnell, Scattering of conduction electrons by localized surface charges, Phys. Rev. 147 (1966) 599.
[9] V.D. Borman, S.Yu. Krylov, A.V. Chayanov, Theory of nonequilibrium phenomena at a gas-solid interface, Sov. Phys. JETP 67 (10) (1988).
[10] S. Brull, P. Charrier, L. Mieussens, Gas-surface interaction and boundary conditions for the Boltzmann equation, Kinet. Relat. Models (2014).
[11] H. Struchtrup, Maxwell boundary condition and velocity dependent accommodation coefficient, Phys. Fluids 25 (2013) 112001.
[12] P. Markowich, C. Ringhofer, C. Schmeiser, Semiconductor Equations, Springer-Verlag, 1990.
[13] M. Lundstrom, Fundamentals of Carrier Transport, Cambridge University Press, 2000.
[14] C. Jacoboni, P. Lugli, The Monte Carlo Method for Semiconductor Device Simulation, Spring-Verlag, Wien–New York, 1989.
[15] E. Fatemi, F. Odeh, Finite difference solution of Boltzmann equation applied to electron transport in semiconductor devices, J. Comput. Phys. 108 (1993) 209–217.

[16] A. Majorana, R. Pidatella, A finite difference scheme solving the Boltzmann Poisson system for semiconductor devices, J. Comput. Phys. 174 (2001) 649–668.
[17] J.A. Carrillo, I.M. Gamba, A. Majorana, C.-W. Shu, A WENO-solver for 1D non-stationary Boltzmann–Poisson system for semiconductor devices, J. Comput. Electron. 1 (2002) 365–375.
[18] J.A. Carrillo, I.M. Gamba, A. Majorana, C.-W. Shu, A direct solver for 2D non-stationary Boltzmann–Poisson systems for semiconductor devices: a MESFET simulation by WENO-Boltzmann schemes, J. Comput. Electron. 2 (2003) 375–380.
[19] J.A. Carrillo, I.M. Gamba, A. Majorana, C.-W. Shu, A WENO-solver for the transients of Boltzmann–Poisson system for semiconductor devices. Performance and comparisons with Monte Carlo methods, J. Comput. Phys. 184 (2003) 498–525.
[20] M.J. Caceres, J.A. Carrillo, I.M. Gamba, A. Majorana, C.-W. Shu, Deterministic kinetic solvers for charged particle transport in semiconductor devices, in: C. Cercignani, E. Gabetta (Eds.), Transport Phenomena and Kinetic Theory Applications to Gases, Semiconductors, Photons, and Biological Systems, in: Modeling and Simulation in Science, Engineering and Technology, Birkhäuser, 2006, pp. 151–171.
[21] J.A. Carrillo, I.M. Gamba, A. Majorana, C.-W. Shu, 2D semiconductor device simulations by WENO-Boltzmann schemes: efficiency, boundary conditions and comparison to Monte Carlo methods, J. Comput. Phys. 214 (2006) 55–80.
[22] M. Galler, A. Majorana, Deterministic and stochastic simulation of electron transport in semiconductors, Bull. Inst. Math. Acad. Sin. (N.S.) 2 (2) (2007) 349–365, 6th MAFPD (Kyoto) special issue.
[23] Z. Chen, B. Cockburn, C. Gardner, J. Jerome, Quantum hydrodynamic simulation of hysteresis in the resonant tunneling diode, J. Comput. Phys. 274 (1995) 274–280.
[24] Z. Chen, B. Cockburn, J.W. Jerome, C.-W. Shu, Mixed-RKDG finite element methods for the 2-d hydrodynamic model for semiconductor device simulation, VLSI Des. 3 (1995) 145–158.
[25] Y.-X. Liu, C.-W. Shu, Local discontinuous Galerkin methods for moment models in device simulations: formulation and one dimensional results, J. Comput. Electron. 3 (2004) 263–267.
[26] Y.-X. Liu, C.-W. Shu, Local discontinuous Galerkin methods for moment models in device simulations: performance assessment and two dimensional results, Appl. Numer. Math. 57 (2007) 629–645.
[27] Y. Cheng, I.M. Gamba, A. Majorana, C.-W. Shu, Discontinuous Galerkin solver for the semiconductor Boltzmann equation, in: T. Grasser, S. Selberherr (Eds.), SISPAD 07, Springer, 2007, pp. 257–260.
[28] Y. Cheng, I. Gamba, A. Majorana, C.-W. Shu, Discontinuous Galerkin solver for Boltzmann–Poisson transients, J. Comput. Electron. 7 (2008) 119–123.
[29] Y. Cheng, I.M. Gamba, A. Majorana, C.-W. Shu, A discontinuous Galerkin solver for Boltzmann–Poisson systems in nano-devices, Comput. Methods Appl. Mech. Eng. 198 (2009) 3130–3150.
[30] Y. Cheng, I.M. Gamba, A. Majorana, C.W. Shu, A discontinuous Galerkin solver for full-band Boltzmann–Poisson models, in: IWCE13, 13th International Workshop on Computational Electronics, 2009.
[31] Y. Cheng, I.M. Gamba, J. Proft, Positivity-preserving discontinuous Galerkin schemes for linear Vlasov–Boltzmann transport equations, Math. Comput. 81 (2012) 153–190.
[32] B. Cockburn, C.-W. Shu, TVB Runge–Kutta local projection discontinuous Galerkin finite element method for conservation laws II: general framework, Math. Comput. 52 (1989) 411–435.
[33] B. Cockburn, S.-Y. Lin, C.-W. Shu, TVB Runge–Kutta local projection discontinuous Galerkin finite element method for conservation laws III: one dimensional systems, J. Comput. Phys. 84 (1989) 90–113.
[34] B. Cockburn, S. Hou, C.-W. Shu, The Runge–Kutta local projection discontinuous Galerkin finite element method for conservation laws IV: the multidimensional case, Math. Comput. 54 (1990) 545–581.
[35] B. Cockburn, C.-W. Shu, The Runge–Kutta local projection P1-discontinuous Galerkin finite element method for scalar conservation laws, Math. Model. Numer. Anal. 25 (1991) 337–361.
[36] B. Cockburn, C.-W. Shu, The Runge–Kutta discontinuous Galerkin method for conservation laws V: multidimensional systems, J. Comput. Phys. 141 (1998) 199–224.
[37] B. Cockburn, C.-W. Shu, Runge–Kutta discontinuous Galerkin methods for convection-dominated problems, J. Sci. Comput. 16 (2001) 173–261.
[38] B. Cockburn, C.-W. Shu, The local discontinuous Galerkin method for time-dependent convection–diffusion systems, SIAM J. Numer. Anal. 35 (1998) 2440–2463.
[39] D. Arnold, F. Brezzi, B. Cockburn, L. Marini, Unified analysis of discontinuous Galerkin methods for elliptic problems, SIAM J. Numer. Anal. 39 (2002) 1749–1779.
[40] C. Cercignani, I.M. Gamba, C.L. Levermore, A drift-collision balance asymptotic for a Boltzmann–Poisson system in bounded domains, SIAM J. Appl. Math. 61 (6) (2001) 1932–1958.